Topical research on nuclear structure, phase transitions and double beta decay

Project code: PCE-ID-2/5.10.2011

Director: Prof. Dr. A. A. Raduta

Synthesizing REPORT, 2011-2016

Team members 1. Prof. Dr. Apolodor Raduta, CSI

2. Dr. Alexandru Raduta, CS I
3. Dr. Cristian Raduta, CS II
4. Dr. Ioan Ursu, CS II
5. Dr. Radu Budaca, CS III
6. Dr. Petrica Buganu, CS III

A. Excellence indicators

Since the project begin several scientific papers have been published either in international journals having big impact factors or in conferences proceedings. Two papers are under evaluation. The list of papers achieved within the mentioned project is given below:

1) New theoretical results for 2 decay within a fully renormalized proton-neutron random-phase approximation approach with the gauge symmetry restored, C. M. Raduta, A. A. Raduta and I. I. Ursu, PHYSICAL REVIEW C 84, 064322 (2011).

2)Semi-microscopic description of back-bending phenomena in some deformed even-even nuclei, A. A. Raduta and R. Budaca, PHYSICAL REVIEW C 84, 044323 (2011).

3)Exact results for the particle-number-projected BCS approach with isovector proton-neutron pairing,A. A. Raduta, M. I. Krivoruchenko, and Amand Faessler, PHYSICAL REVIEW C 85, 054314 (2012).

4)Interplay of classical and quantal features within the coherent-state model, A. A.

Raduta and C. M. Raduta, PHYSICAL REVIEW C 86, 054307 (2012).

5)FRpnQRPA approach with the gauge symmetry restored. Application for the 2 decay, A. A. Raduta and c. M. Raduta, EPJ Web of Conferences 38, 14003 (2012).

6)FRpnQRPA APPROACH WITH THE GAUGE SYMMETRY RESTORED. APPLICATION FOR THE 2 DECAY , A. A. Raduta,(c) Rom.Journ. Phys., Vol.57,nr. 1-2, pp. 442-471, 2012

7) Semi-microscopic description of the double back-bending in some deformed even-even rare earth nuclei, R Budaca and A A Raduta, J. Phys. G: Nucl. Part. Phys. 40 (2013) 025109 (26pp).

8) Application of the sextic oscillator with a centrifugal barrier and the spheroidal equation for some X(5) candidate nuclei, A A Raduta and P Buganu, J. Phys. G: Nucl. Part. Phys. 40 (2013) 025108 (29pp).

9) $2\nu\beta\beta$ decay within a higher pnQRPA approach with the gauge symmetry preserved, A. A. Raduta, and C. M. Raduta, Journal of Physics: Conference Series 413 (2013) 012014.

10) A semi-microscopic approach to the back-bending phenomena in even-even nuclei,A A Raduta and R Budaca,Journal of Physics: Conference Series 413 (2013) 012028.

11) Towards a new solvable model for the even-even triaxial nuclei, A. A. Raduta and P. Buganu,Journal of Physics: Conference Series 413 (2013) 012029.

12) Description of the isotope chain 180-196Pt within several solvable approaches,A. A. Raduta, P. Buganu, Phys. Rev. C 88 (2013) 064328.

13) Deformation properties of the projected spherical single particle basis, A.A. Raduta, R. Budaca, Annals of Physics 347 (2014) 141169.

14)A new picture for the chiral symmetry properties within a particlecore framework A Raduta, C M Raduta and Amand Faessler,Jour. Phys. G: Nucl. Part. Phys. 41 (2014) 035105 (27pp), doi:10.1088/0954-3899/41/3/035105.

15) Harmonic oscillator potential with a sextic anharmonicity in the prolate -rigid collective geometrical model, R. Budaca,Physics Letters B 739 (2014) 5661.

16) Quartic oscillator potential in the -rigid regime of the collective geometrical model, R. Budaca, Eur. Phys. J. A (2014) 50: 87; DOI 10.1140/epja/i2014-14087-8

17) Semi-microscopic description of the proton- and neutron-induced back-bending phenomena in some deformed even-even rare earth nuclei R. Budaca and A. A. Raduta, EPJ Web of Conferences 66, 02017 (2014), DOI: 10.1051/epjconf/ 201 4 6602017

18) Application of the sextic oscillator potential together with Mathieu and spheroidal functions for triaxial and X(5) type nuclei, A. A. Raduta and P. Buganu, EPJ Web of Conferences 66, 02086 (2014), DOI: 10.1051/epjconf/ 201 4 66020 86

19) Description of the chiral bands in 188,190 Os, A. A. Raduta and C. M. Raduta, submitted to Physics Letters B.

20) Analytical solution for the Davydov-Chaban Hamiltonian with sextic potential for $\gamma = 30^0$, P. Buganu and R. Budaca, submitted to Physical Review C 91 (2015) 014306

21) Semi-phenomenological description of the chiral bands in 188;190Os, A. A. Raduta and C. M. Raduta, J. Phys. G: Nucl. Part. Phys. 42 (2015) 065105 (16pp)

22) ENERGY SPECTRA, E2 TRANSITION PROBABILITIES AND SHAPE DEFORMATIONS FOR THE EVEN-EVEN ISOTOPES 180196 Pt,P. BUGANU1 , A.A. RADUTA1,2,Rom.Journ. Phys., Vol. 60, Nos.1-2, (2015) p. 161-178.

23) Nuclear Structure with coherent states, Apolodor Aristotel Raduta, Book, 521 pagini, Springer, Heidelberg, New York, London, ISBN 978-3-319-14641-6, DOI 10. 1007/978-3-319-14642-3

24) A new renormalization procedure of the quasiparticle random phase approximation, A. A. Raduta and C. M. Raduta, Int. Jour. Mod. Phys. E **25**, No. 3 (2016) 1650017.

25) Specific features and symmetries for magnetic and chiral bands in nuclei, A. A. Raduta, Progress in Particle and Nuclear Physics **90** (2016) 241-298.

B.Important results, activities

RESULTS, 2011

Stage 1: Double beta decay and the backbending henomenon

I. A many body Hamiltonian including a mean field corresponding to a projected spherical single particle basis, pairing interaction of alike nucleons, a repulsive proton-neutron dipole-dipole interaction acting in the particle-hole (ph) channel and an attractive proton-neutron interaction of particle-particle type is treated in the framework of **a formalism where the gauge symmetry is restored and the pnQRPA approach is fully renormalized**. Energies and wave functions have been used to calculate the decay rates and half-life's for the following isotopes: ^{48}Ca, ^{76}Ge, ^{82}Se, ^{96}Zr, ^{104}Ru, ^{110}Pd, ^{128,130}Te, ^{148,150}Nd, ^{154}Sm, and ^{160}Gd.

Results were compared with experimental data as well as with the theoretical calculations performed with other models. We mention that for all cases considered the Ikeda sum-rule is obeyed. In fact this is a distinctive merit of our work. We also studied the β^- strength for the mother nuclei and the β^+ strength characterizing the daughter nuclei as function of the $GRFRpnQRPA$ energies. For few cases the available experimental data are presented.

It is worth mentioning that without exception the double beta emitters are stable with respect to the single beta decay. However the intermediate odd-odd nuclei may decay through β^- to the corresponding daughter nuclei of the $2\nu\beta\beta$ process or may go to the mother nuclei through an electron capture process which is equivalent to a β^+ decay. For such nuclei the log ft for both decays were calculated and results compared with the experimental data. Moreover one suggests that the attractive interaction strength be determined by fitting one of the two log ft mentioned above. Also the total strengths for the β^- and β^+ decays were calculated. For few nuclei there are available data concerning the mentioned observable. We mention the fact that for all nuclei considered here the agreement between the predictions of the present formalism and the experimental data is very good.

We underline the fact that our formalism is the only one which describes simultaneously the double beta amplitude and the Ikeda sum rule. The said sum rule asserts that the difference between the total β^- strength and the total β^+ strength is equal to 3(N-Z) where N and Z are the neutron and proton numbers respectively.

II. Another subject treated within our project refers to the back-bending phenomena. For regular spectra the energy spacing of the consecutive levels is an increasing function of the state angular momentum. If for a certain angular momentum the monotonic feature of the energy spacing is broken this is reflected in the plot of the moment of inertia vs the rotational frequency squared by that the ascendent curve is bending back. The sudden banding of the mentioned curve is caused by an discontinuous increase of the moment of inertia. This variation might be determined by a transition from a super-fluid to a normal phase. Such a transition can be induced by breaking of a neutron pair near the Fermi sea. The pairs breaking is determined by a term which breaks the time reversal symmetry. The new feature of the proposed approach consists of that the nucleons move around a phenomenological deformed core in deformed orbits.

Thus, the back-bending mechanism was studied in terms of two bands hybridization. These bands are obtained by treating a hybrid system with two components: a set of par-

ticles moving in a deformed mean field and a phenomenological core whose ground state is described by an axially symmetric coherent state for quadrupole bosons. The two components interact with each other by a quadruole-quadrupole term and a spin-spin force. The total Hamiltonian is analyzed in a space of states of good angular momentum obtained through projection from deformed product functions.

The factor function associated to the single particle motion defines the rotational band nature. The ground band has all particles paired while that of two quasiparticles type is built upon a neutron broken pair in an intruder state, that is of large angular momentum, $i_{13/2}$. Theory was applied to six nuclei from the rare earth region. An excellent agreement with experimental data has been obtained.

RESULTS, 2012

Stage 2: New results for CSM;
The double beta transition to excited states within GRFRpnQRPA

I. DESCRIPTION OF THE PHASE TRANSITION $O(6) \rightarrow SU(5)$ WITHIN CSM. THE RELATION TO OTHER DESCRIPTIONS

The present work belongs to a series of publication authored by the team members [1–5], and devoted to the study of phase transition in even-even nuclei. Nuclear phases corresponding to the symmetries U(5) (spherical oscillator), SU(3) (symmetrical rotor) and O(6) ($\gamma-$unstable) are associated shapes of nuclei staying in the ground state, namely spherical, symmetric and asymmetric respectively. They are described in terms of the intrinsic deformations β and γ [1]. The main results reported in this field were reviewed in Refs. [7, 8].

The aim of our investigation was the description of the even-even nuclei which represent the critical point in the transition $U(5) \rightarrow SU(3)$. The harmonic potential in the variable β was replaced with a sextic one plus a centrifugal term while the potential in γ is a periodic function. By the variable separation method the coupled differential equation in the two deformations is separated. The equation for β is quasi-exactly solvable while that in γ admits the spheroidal functions as solution. The two equations provide the energies carried by the two degrees of freedom and therefore the system total energy. The resulting wave function

is further used together with an anharmonic transition operator, for calculating the reduced E2 transition probabilities. The approach formulated above was conventionally called Sextic and Spheroidal Approach (SSA). SSA was applied for ten nuclei, namely ^{176,178,180,188,190}Os, ^{150}Nd, ^{170}W, ^{156}Dy, ^{166,168}Hf. These nuclei have the energy ratio for the first two excited states in the ground band close to 2.9. This feature is considered to be a signature for the so called $X(5)$ symmetry [2]. The agreement between our calculations and the corresponding experimental data is very good. The SSA results were also compared with those obtained by different approaches: X(5) [2], an infinite 5D square well(ISW) [1], Davidson potential (D) [2] and the coherent state model (CSM) Model [5]. One concludes that SSA is an simple an efficient tool for describing the nuclei which realize the critical point of the phase transition $U(5) \to SU(3)$.

Comparing the r.m.s. (root mean square) values provided by the mentioned formalisms one noticed that for ^{180}Os, ^{150}Nd and ^{170}W the CSM description is better while for ^{188}Os the SSA descriptions is the most appropriate one. For the remaining nuclei the model D produces results which are closest to the experimental data.

Concerning the e.m. transitions, for ^{176,178,180}Os, ^{166,168}Hf and ^{170}W only data for the intraband transitions characterizing the ground band are available while for remaining nuclei data concerning interband transitions are also known. The five approaches considered in our paper predict values for the available rates close to the corresponding experimental data.

The final conclusion is that SSA is an adequate approach to describe the critical point of the transition $U(5) \to SU(3)$.

The results which were shortly described above were included in the work: *Application of the sextic oscillator with centrifugal barrier and the spheroidal equation for some X(5) candidate nuclei*, A. A. Raduta and P. Buganu, Journal of Physics G: Nuclear and Particle Physics, J. Phys. G: Nucl. Part. Phys. 40 (2013) 025108 (29pp).

---

[1] A. Gheorghe, A. A. Raduta and A. Faessler, Phys. Lett. **B 648**, (2007) 171.

[2] A. A. Raduta, A. C. Gheorghe, P. Buganu and A. Faessler, Nucl. Phys. **A 819**, (2009) 46.

[3] A. A. Raduta and P. Buganu, Phys. Rev. **C 83**, (2011) 034313.

[4] P. Buganu and A. A. Raduta, J. Phys. G: Nucl. Part. Phys. **39** (2012) 025103.

[5] P. Buganu and A. A. Raduta, Rom. Journ. Phys. **57** (2012) 1103.

[6] A. Bohr, Mat. Fys. Medd. Dan. Vid. Selsk. **26** (1952) no.14; A.Bohr and B.Mottelson, Mat. Fys. Medd. Dan. Vid. Selsk. **27** (1953) no. 16

[7] L. Fortunato, Eur. J. Phys. **A 26**, s01, 1-30 (2005).

[8] P. Cejnar, J. Jolie and R. F. Casten, Rev. Mod. Phys. **82**, No. 3 (2010).

[9] F. Iachello, Phys. Rev. Lett. **87** (2001) 052502.

[10] A. A. Raduta, V. Ceausescu, A. Gheorghe and R. M. Dreizler, Phys. Lett. **99B** (1981) 444; Nucll. Phys. **A381** (1982) 253.

[11] Balraj Singh,Nuclear Data Sheets **95**, 387 (2002).

II. ASYMPTOTIC AND NEAR VIBRATIONAL BEHAVIOR OF THE CSM APPROACH. THE RELATION TO OTHER DESCRIPTIONS.

Since the liquid drop model (LDP) was emitted [1] many authors have used the quadrupole coordinates both in phenomenological models and microscopic formalisms, in order to explain the basic properties of complex nuclei [2]. LDP as proposed by Bohr and Mottelson is able to describe only few properties of the spherical nuclei. Faessler and Greiner extended the LDP making it suitable also for the description of deformed nuclei. The resulting formalism, called the Rotation Vibration Model (RVM), was further extended by including in the model Hamiltonian anharmonic terms which are polynomial invariants in the quadrupole coordinates. The main drawback of this approach is the large number of adjustable parameters. By contrast to RVM, the coherent state model (CSM) [3] uses a much less parameters. The salient feature of the CSM is that it describes, in a realistic fashion, nuclei ranging from transitional to well deformed region with spins running from low up to high and even very high values. The space of model states associated to a given angular momentum is three dimensional. The states are obtained through angular momentum projection from three orthogonal deformed states among which one is an axially deformed coherent state of Glauber type constructed with the zeroth component of the quadrupole boson. This describes the ground state of the nuclear system. The remaining two deformed states are the lowest order polynomial excitations of the ground state which are chosen such that the functions are orthogonal onto each other both before and after the angular momentum projection. The expressions of the model states are:

$$
\begin{aligned}
\phi^g_{JM}(d) &= N^g_J P^J_{M0}\psi_g, \quad \psi_g = \exp\left[d(b^\dagger_0 - b_0)\right]|0\rangle, \\
\phi^\beta_{JM}(d) &= N^\beta_J P^J_{M0}\Omega^\dagger_\beta\psi_g, \quad \Omega^\dagger_\beta = \left(b^\dagger b^\dagger b^\dagger\right)_0 + \frac{3d}{\sqrt{14}}\left(b^\dagger b^\dagger\right)_0 - \frac{d^3}{\sqrt{70}}, \\
\phi^\gamma_{JM}(d) &= N^\gamma_J P^J_{M2}\Omega^\dagger_{\gamma,2}\psi_g, \quad \Omega^\dagger_{\gamma,m} = \left(b^\dagger b^\dagger\right)_{2,m} + d\sqrt{\frac{2}{7}}b^\dagger_m.
\end{aligned} \tag{1}
$$

The parameter d plays the role of the nuclear deformation. Within this restricted collective states one considered an effective Hamiltonian satisfying the restriction of being maximally decoupled. A possible solution is the following sixth order boson Hamiltonian.

$$
H = A_1(22\hat{N} + 5\Omega^\dagger_{\beta'}\Omega_{\beta'}) + A_2\hat{J}^2 + A_3\Omega^\dagger_\beta\Omega_\beta, \quad \Omega^\dagger_{\beta'} = \left(b^\dagger b^\dagger\right)_0 + \frac{d^2}{\sqrt{5}}. \tag{2}
$$

A nice property of the CSM is that the state norms as well as the matrix elements of the effective Hamiltonian can be expressed in terms of one overlap integral and its first derivative:

$$
I^{(0)}_J(d^2) = \int_0^1 P_J(y)e^{d^2P_2(y)}dy, \quad I^{(k)}_J(x) = \frac{d^k I^{(0)}_J}{dx^k}, \quad x = d^2. \tag{3}
$$

For the overlap integral an analytical expression is possible and therefore the energies of the ground, β and γ bands as well as the transition rates could be analytically calculated. Moreover these expressions are particularly simple when the deformation parameter d is either in the near vibrational interval or in the asymptotic region [4]. For example in the later case we have:

$$
\begin{aligned}
E^g_J &= 11A_1\left[\frac{x-1}{2} + \sqrt{G_J}\right] + A_2J(J+1), \ x = d^2, \\
E^\beta_J &= \frac{1}{P^\beta_J}\left[A_1S^\beta_J + A_3F^\beta_J\right] + A_2J(J+1), \\
E^\gamma_J &= A_1\frac{S^\gamma_J}{P^\gamma_J} + A_2J(J+1).
\end{aligned} \tag{4}
$$

P, S, F and G are polynomials in $1/x$ with coefficients depending on the angular momentum. Similarly the matrix element of the transition operator can be expressed as:

$$
\begin{aligned}
\langle\phi^i_J||Q^h_2||\phi^i_{J'}\rangle &= 2dq_hC^{J\,2\,J'}_{K_i0\,K_i}, \quad i = g,\beta,\gamma, \quad K_i = -2\delta_{i\gamma}, \\
\langle\phi^\gamma_J||Q^h_2||\phi^g_{J'}\rangle &= \sqrt{2}q_hC^{J\,2\,J'}_{-2\,2\,0}, \\
\langle\phi^\beta_J||Q^h_2||\phi^\gamma_{J'}\rangle &= \frac{2}{3\sqrt{19}}q_hC^{J\,2\,J'}_{0\,-2\,-2}, \ \langle\phi^\beta_J||Q^{anh}_2||\phi^g_{J'}\rangle = 2\sqrt{\frac{7}{19}}q_{anh}C^{J\,2\,J'}_{0\,0\,0}.
\end{aligned} \tag{5}
$$

Note the the matrix element from above depend on angular momentum through a Clebsch Gordan coefficient which is consistent with the so called Alaga rule.

As for the near vibrational regime, expanding the overlap integrals in series of $x = d^2$, energies become rational function of x with the coefficients involved depending on $J(J+1)$.

$$
\begin{aligned}
E_J^g &= 22A_1 \sum_{k=0}^{3} A_{J,k}^{(g)} x^k + A_2 J(J+1) - \Delta E_J, \\
E_J^\gamma &= 44A_1 + \frac{A_1}{\sum_{k=0}^{3} Q_{J,k}^{(\gamma,0)} x^k} \left[\sum_{k=0}^{3} \left(22R_{J,k}^{(\gamma,0)} + 5U_{J,k}^{(\gamma,0)} \right) x^k \right] + A_2 J(J+1) + \Delta E_J,\ J = par, \\
E_J^\gamma &= 44A_1 + \frac{A_1}{\sum_{k=0}^{3} Q_{J,k}^{(\gamma,1)} x^k} \left[\sum_{k=0}^{3} \left(22R_{J,k}^{(\gamma,1)} + 5U_{J,k}^{(\gamma,1)} \right) x^k \right] + A_2 J(J+1),\ J = impar, \\
E_J^\beta &= \frac{1}{\sum_{k=0}^{3} Q_{J,k}^{(\beta)} x^k} \left\{ A_1 \sum_{k=0}^{3} \left(22R_{J,k}^{(\beta)} + 5U_{J,k}^{(\beta)} \right) x^k + \sum_{k=0}^{3} \left(A_3 V_{J,k}^{(\beta)} + A_4 dZ_{J,k}^{(\beta)} + A_5 B_{J,k}^{(\beta)} \right) x^k \right\} + A_2 J(J+1).
\end{aligned}
\tag{6}
$$

The coefficients A, R, U, V, Z, B and the correction ΔE are ratios of polynomials in $J(J+1)$. Analogously the reduced transition probabilities can be also analytically expressed.

In the vibrational limit the projected states become multi-phonon states and consequently the analytical expressions leads at some selection rules for the E2 transitions. For a certain choice of the parameters involved in the model Hamiltonian the surface of constant energy exhibit minima which may be associated to equilibrium shapes like: spherical, axially prolate or oblate and triaxial. To each equilibrium shape correspond specific properties reflected both in excitation energies and transition probabilities, which in fact define the nuclear phase. Moreover, each nuclear shape exhibits a certain symmetry and therefore the associated properties might be described by the irreducible representations of the underlying group of transformations [5]. In this context the CSM was used to simultaneously describe three interacting bands, ground, beta and gamma, in 42 nuclei [6] belonging to different symmetries like $SU(5)$, $O(6)$, $SU(3)$, and triaxial shapes or to the transitional regions between two extreme limits. Numerical results agree very well with the corresponding experimental data. How do we distinguish the nuclear phases. Indicators for the the regime to which a chosen nucleus accommodates are the ratio $R = E_{4_1^+}/E_{2_1^+}$ and the deformation parameter d. For example in the near vibrational limit R is close to 2 and d is less than the convergence radius of the overlap integral $I_J^{(0)}$ [7]. The 42 nuclei, treated in our paper, can be divided in three categories: strongly deformed transuranic, near vibrational, deformed from the rare earth region. The parameters involved in the model Hamiltonian and the deformation pa-

rameter d were determined through the least square procedure. The obtained values of the optimal parameters as well as of energies and transition probabilities allow us to include the chosen nucleus to one category or another. For each category of nuclei one notices that the deformation parameter d depend linearly on the nuclear deformation β. Moreover the three lines are more or less parallel. Concerning the structure coefficients they do not change chaotically when one passes from one nucleus to another. For each category, they can be interpolated by low order polynomials in $A + (N - Z)/2$. It is worth noting that the nuclei whose parameters substantially differ from the point of the interpolating curve are critical points for phase transitions $(X(5), E(5), Y(5))$. This is best seen for the isotopic chain of Gd where two such transitions are identified.

The results which were briefly presented above are in extenso described in the publication: *Analytical description of the coherent state model for the near vibrational and well deformed nuclei*, A. A. Raduta, R. Budaca, A. Faessler, Ann. Phys. (NY) **327** (2012) 671.

---

[1] A. Bohr, Mat. Fys. Medd. Dan. Vid. Selsk. **26** (1952) no.14; A.Bohr and B.Mottelson, Mat. Fys. Medd. Dan. Vid. Selsk. **27** (1953) no. 16.

[2] A. Faessler and W. Greiner, Z. Phys. **168** (1962) 425; **170** (1962) 105; **177** (1964) 190; A. Faessler, W. Greiner and R. Sheline, Nucl. Phys. **70** (1965) 33.

[3] A. A. Raduta, V. Ceausescu, A. Gheorghe and R. M. Dreizler, Phys. Lett. **99B** (1981) 444; Nucl. Phys. **A381** (1982) 253.

[4] A. A. Raduta and C. Sabac, Ann. Phys. (N.Y.) **148** (1983) 1.

[5] F. Iachello and A. Arima, *The Interacting Boson Model* (Cambridge University Press, Cambridge, England, 1987).

[6] A. A. Raduta, R. Budaca, A. Faessler, Ann. Phys. (NY) **327** (2012) 671.

[7] A. A. Raduta, R. Budaca, A. Faessler, Jour. Phys. G: Nucl. Part. Phys. **37** (2010) 085108.

[8] R. Budaca, A. A. Raduta, Rom. Journ. Phys. **57** (2012) 1088.

III. QUANTUM VS CLASSICAL FEATURES IN NUCLEAR SYSTEMS

The CSM has the peculiarity that it uses a restricted boson space defined by angular momentum projection from three orthogonal states one of them being a coherent state while the other are polynomial excitations of the first. The three projected states are model states for the ground, β and γ bands. The coherent state has the property that it minimizes the uncertainty relations for the quadrupole coordinate and its conjugate momentum. This property is considered to define the border between the classical and quantum mechanical behavior of the system. On the other hand the coherent state violates the gauge and rotation symmetries. The departure of the uncertainty relations from the classical limit is considered to be a measure for the quantal behavior. This measure was analyzed both in the vibrational and the asymptotic limits. We tried also to answer the question: *What is the role of nuclear deformation in determining the classical or quantal behavior of the nuclear system.* Another feature which were in detail discussed is whether the answer to the above question depends on the chosen pair of conjugate coordinate and momentum. We didn't provide a general solution to this problem but rather considered two independent pairs of conjugate coordinate and momentum: the quadrupole coordinate and the conjugate momentum, the boson number and the conjugate phase. Such features are studied in the publication:

Interplay of classical and quantal features within the coherent state model, A. A. Raduta and C. M. Raduta, PHYSICAL REVIEW C 86, 054307 (2012).

---

[1] M. Baranger and M. Veneroni, Ann. Phys. (NY) **114**, 123 (1978).

[2] F. Villars, Nucl. Phys. **A285**, 269 (1977).

[3] A. A. Raduta, V. Baran and D. S. Delion, Nucl. Phys. **A588**, 431 (1995).

[4] A. A. Raduta, R. Budaca and Amand Faessler, Jour. Phys. G: Nucl. Part. Phys. **38**, 055102 (2011).

[5] A. A. Raduta and R. M. Dreizler, Nucl. Phys. **A258**, 109 (1976).

[6] A. A. Raduta, V. Ceausescu, A. Gheorghe and R. M. Dreizler, Nucl. Phys. **A381**, 253 (1982).

[7] P. Haapakoski, T. Honkaranta and P. O. Lipas, Phys. Lett. **41 B**, 125 (1970).

[8] P. A. M. Dirac, Proc. Roy. Soc. (London) **A114**, 243 (1927).

[9] L. Susskind and J. Glogow, Physics **1**, 49 (1964).

[10] P. Carruthers and Michael Martin Nieto, Rev. Mod. Phys. **40**, 411 (1968).

[11] W. H. Louisell, Phys. Lett. **7**, 60, (1963).

[12] P. Carruthers and M. M. Nieto, Phys. Rev. Lett. **14**, 387 (1965).

[13] R. D. Levine, The Journal of Chemical Physics, **44**, 3597 (1965).

[14] A. A. Raduta, R. Budaca and Amand Faessler, Ann. Phys.[NY] **327**, 671 (2012).

[15] A.S. Holevo, *Probabilistic and Statistical Aspects of Quantum Theory,* 2nd edition, Edizioni della Normale, Pisa, 2011, ISBN: 978-88-7642-375-8 Nauka, Moscow, 1980, Russian translation, pp. 204-211.

RESULTS, 2013

Stage 3: Phase transition; The SSD hypothesis

1. A new picture for the chiral symmetry properties within a particle-core framework,A. A. Raduta, C. M. Raduta and Amand Faessler, Journal of Physics G; Nucl. Part. Phys.41 (2014) 035105 (27pp)

Rotational spectra appear to be a reflection of a symmetry spontaneous breaking which results of having a static deformation for the nuclear system. Some of the fundamental properties of nuclear systems may be evidenced through their interaction with an electromagnetic field. The two components of the field, electric and magnetic, are used to explore the properties of electric and magnetic nature, respectively. At the end of last century the scissors like states [1–3] as well as the spin-flip excitations [4] have been widely treated by various groups. Some of them were based on phenomenological assumptions while the other ones on microscopic considerations. The scissors like modes are excited in (e,e') experiments at backward angles and expected at an energy of about 2-3 MeV, while the spin-flip excitations are seen in (p,p') experiments at forward angles and are located at about 5-10 MeV. The scissors mode describes the angular oscillation of proton against neutron system and the total strength is proportional to the nuclear deformation squared which reflects the collective character of the excitation [3, 4].

In virtue of this feature it was believed that the magnetic collective properties are in general associated with deformed systems. This is not true due to the magnetic dipole bands, where the ratio between the moment of inertia and the B(E2) value for exciting the first 2^+ from the ground state 0^+, $\mathcal{I}^{(2)}/B(E2)$, takes large values, of the order of $100(\text{eb})^{-2}MeV^{-1}$. These large values can be justified by a large transverse magnetic dipole moment which induces dipole magnetic transitions, but almost no charge quadrupole moment [1]. Indeed, there are several experimental data showing that the dipole bands have large values for $B(M1) \sim 3-6\mu_N^2$, and very small values of $B(E2) \sim 0.1(eb)^2$ (see for example Ref.[6]). The states are different from the scissors mode, they being rather of a shears character. A system with a large transverse magnetic dipole moment may consist of a triaxial core to which a proton prolate and a neutron oblate hole orbital are coupled. The interaction of particle and hole like orbitals is repulsive, which keeps the two orbits apart from each other. In this way the orthogonal angular momenta carried by the proton particles and neutron holes are favored. The maximal transverse dipole momentum is achieved, for example, when $\mathbf{j_p}$ is oriented along the small axis of the core, $\mathbf{j_n}$ along the long axis and the core rotates around the intermediate axis. Suppose the three orthogonal angular momenta form a right trihedral frame. If the Hamiltonian describing the interacting system of protons, neutrons and the triaxial core is invariant to the transformation which changes the orientation of one of the three angular momenta, i.e. the right trihedral frame is transformed to a left type, one says that the system exhibits a chiral symmetry. As always happens, such a symmetry is identified when that is broken and consequently to the two trihedral-s correspond distinct energies, otherwise close to each other. Thus, a signature for a chiral symmetry characterizing a triaxial system is the existence of two $\Delta I = 1$ bands which are close in energies. Increasing the total angular momentum, the gradual alignment of $\mathbf{j_p}$ and $\mathbf{j_n}$ to the total $\mathbf{J}$ takes place and a magnetic band is developed. The question which naturally arise is whether the proposed solution for chiral band is unique. Also note that so far only the odd-odd nuclei were investigated. In the recent past the magnetic states of spin-flip type have been studied by several groups [1–10]. Our group studied the dipole bands having $K^\pi = 1^\pm$ with a Hamiltonian describing the interaction of quadrupole and octupole bosons [11]. We have shown the the band 1^+ is of a magnetic nature while the band 1^- has an electric character. In an other publication [18] we have noticed that for parity partner bands starting with a critical angular momentum the angular momenta carried b the quadrupole and octupole

bosons are orthogonal. It is expected that adding to such a system a set of nucleons we can find a suitable strength for the particle core interaction such that the angular momentum of nucleons is perpendicular on the plane of quadrupole and octupole angular momenta. As we said before such a configuration is a prerequisite for the existence of a chiral band. The first attempt of this kind was achieved in Ref.[19].

Here we attempt another chiral system consisting of one phenomenological core with two components, one for protons (of angular momentum $\mathbf{J}_p$) and one for neutrons (of angular momentum $\mathbf{J}_n$), and two quasiparticles whose total angular momentum $\mathbf{J}$ is oriented along the symmetry axis of the core due to the particle-core interaction. In a previous publication we proved that states of total angular momentum $\mathbf{I}$, where the three components mentioned above carry the angular momenta $\mathbf{J}_p, \mathbf{J}_n, \mathbf{J}$ which are mutually orthogonal, do exist. Such configuration seems to be optimal to define large transverse magnetic moment inducing large M1 transitions.

In what follows we shall briefly review the main ingredients of the proposed phenomenological formalism. The Hamiltonian which describe the particle-core system is:

$$\begin{aligned} H &= H_{GCSM} + \sum_{\alpha} \epsilon_a c_\alpha^\dagger c_\alpha - \frac{G}{4} P^\dagger P \\ &- \sum_{\tau=p,n} X_{pc}^{(\tau)} \sum_m q_{2m} \left(b_{\tau,-m}^\dagger + (-)^m b_{\tau m} \right) (-)^m - X_{sS} \vec{J}_F \cdot \vec{J}_c, \end{aligned} \tag{1.1}$$

The quadrupole moment is denoted as follows:

$$\begin{aligned} q_{2m} &= \sum_{a,b} Q_{a,b} \left(c_{j_a}^\dagger c_{j_b} \right)_{2m}, \\ Q_{a,b} &= \frac{\hat{j}_a}{\hat{2}} \langle j_a || r^2 Y_2 || j_b \rangle. \end{aligned} \tag{1.2}$$

Here H_{GCSM} denotes the phenomenological Hamiltonian defining the generalized coherent state model (GCSM) and is associated to a proton and neutron bosonic core. The next two terms stand for a set of particles moving in a spherical shell model mean-field and interacting among themselves through pairing interaction. The low indices α denote the set of quantum numbers labeling the spherical single particle shell model states, i.e. $|\alpha\rangle = |nljm\rangle = |a, m\rangle$. The last two terms denoted hereafter as H_{pc} express the interaction between the satellite particles and the core through a quadrupole-quadrupole and a spin-spin force, respectively.

The angular momenta carried by the core and particles are denoted by $\mathbf{J}_c(=\mathbf{J}_{pn})$ and $\mathbf{J}_F$, respectively.

The mean field plus the pairing term is quasi-diagonalized by means of the Bogoliubov-Valatin transformation. The Hamiltonian has been treated in the restricted space of particle-core states: $\phi^{(g)}_{JM}|BCS\rangle, \phi^{(\beta)}_{JM}|BCS\rangle, \phi^{(\gamma)}_{JM}|BCS\rangle, \phi^{(1)}_{JM}|BCS\rangle, \widetilde{\phi}^{(1)}_{JM}|BCS\rangle$ and $\Psi^{(2qp;J1)}_{JI;M}$ defined as:

$$\begin{aligned}
\phi^{(g)}_{JM} &= N^{(g)}_J P^J_{M0}\psi_g, \quad \psi_g = exp[(d_p b^\dagger_{p0} + d_n b^\dagger_{n0}) - (d_p b_{p0} + d_n b_{n0})]|0\rangle, \\
\phi^{(\beta)}_{JM} &= N^{(\beta)}_J P^J_{M0}\Omega_\beta\psi_g, \\
\phi^{(\gamma)}_{JM} &= N^{(\gamma)}_J P^J_{M2}(b^\dagger_{n2} - b^\dagger_{p2})\psi_g, \\
\phi^{(1)}_{JM} &= N^{(1)}_J P^J_{M1}(b^\dagger_n b^\dagger_p)_{11}\psi_g, \\
\tilde{\phi}^{(1)}_{JM} &= \tilde{N}^{(1)}_J P^J_{M1}(b^\dagger_{n1} - b^\dagger_{p1})\Omega^\dagger_\beta\psi_g, \\
\Psi^{(2qp;J1)}_{JI;M} &= N^{(2qp;J1)}_{JI}\sum_{J'} C^{J\ J'\ I}_{J\ 1\ J+1}\left(N^{(1)}_{J'}\right)^{-1}\left[(a^\dagger_j a^\dagger_j)_J|BCS\rangle \otimes \varphi^{(1)}_{J'}\right]_{IM}. \qquad (1.3)
\end{aligned}$$

The following notations have been used:

$$\begin{aligned}
\Omega^\dagger_{\gamma,k,2} &= (b^\dagger_k b^\dagger_k)_{22} + d_k\sqrt{\frac{2}{7}}b^\dagger_{k2}, \quad k = p, n, \\
\Omega^\dagger_\beta &= \Omega^\dagger_p + \Omega^\dagger_n - 2\Omega^\dagger_{pn}, \\
\Omega^\dagger_k &= (b^\dagger_k b^\dagger_k)_0 - \sqrt{\frac{1}{5}}d^2_k, \quad k = p, n, \\
\Omega^\dagger_{pn} &= (b^\dagger_p b^\dagger_n)_0 - \sqrt{\frac{1}{5}}d^2_p. \\
\hat{N}_{pn} &= \sum_m b^\dagger_{pm} b_{nm},\ \hat{N}_{np} = (\hat{N}_{pn})^\dagger, \quad \hat{N}_k = \sum_m b^\dagger_{km} b_{km},\ k = p, n. \qquad (1.4)
\end{aligned}$$

The state $|BCS\rangle$ is a vacuum state for quasiparticles. The energies in the bands defined by the the wave functions mentioned above are defined as average values of the model Hamiltonian in with a state from the particle-core space. There are several parameters involved which were determined by fitting some energies from the ground, beta and gamma bands. Numerical application refers to ^{192}Pt which is γ soft and triaxial and by this a good candidate for a chiral configuration. The parameters obtained by the mentioned fitting procedure are listed in Table I. There we listed also the values of the parameter

$$X'_{pc} = 6.5\eta^{(-)}_{\frac{11}{2}\frac{11}{2}}\frac{\hbar}{M\omega_0}X^{(p)}_{pc}, \qquad (1.5)$$

$\rho = d\sqrt{2}$	A_1	A_2	A_3	A_4	X'_{pc}	X_{sS}
2.0	555.4	-25.4	-12.8	7.7	-23.4	1.

TABLE I: The structure coefficients determined through the least square procedure, given in keV . The deformation parameter ρ is dimensionless while X'_{pc} is defined by Eq. Eq. (1.5).

Here M and ω_0 the proton mass and the oscillator frequency used in the shell model. Since we considered as satellite nucleons the protons in the shell $h_{11/2}$ we took $X_{pc}^{(n)} = 0$. The excitation energies corresponding to the parameters from Table 1 were compared with the experimental data in Fig. 1. We remark a very good agreement between the two sets of data.

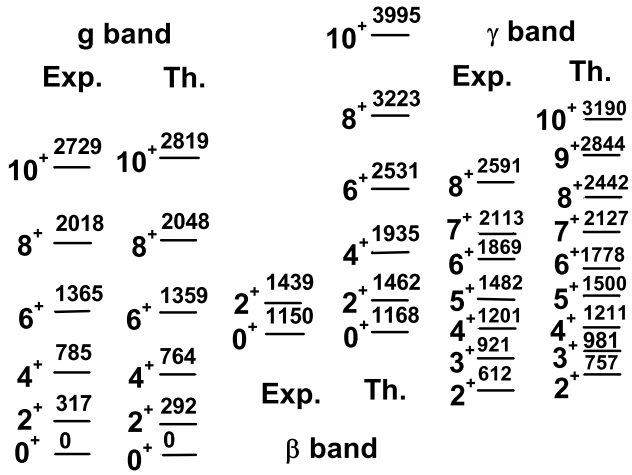

FIG. 1: Experimental and calculated excitation energies in ground, β and γ bands for ^{192}Pt. They correspond to the fitted parameters listed in Table 1. The r.m.s. value of the deviation of the theoretical results and the corresponding experimental data is equal to 67 keV.

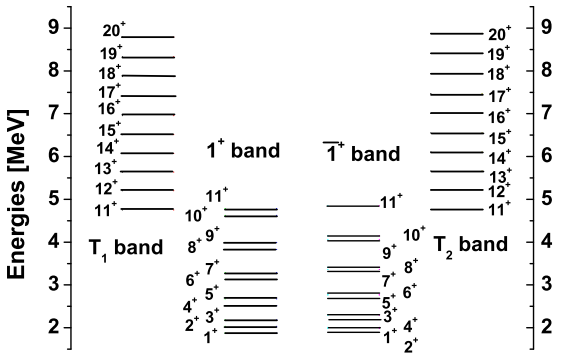

FIG. 2: The excitation energies for the dipole bands described by $\phi^{(1)}_{JM}$ (left lower column) and $\tilde{\phi}^{(1)}_{JM}$ (right lower column), respectively. The bands T_1 (upper left column) and T_2 (upper right column), conventionally called twin bands, are also shown. The T_1 and T_2 bands were obtained with X'_{pc}=-0.023 MeV and X_{sS}= 0.001 MeV for the left column and X_{sS}=-0.001MeV for the right column.

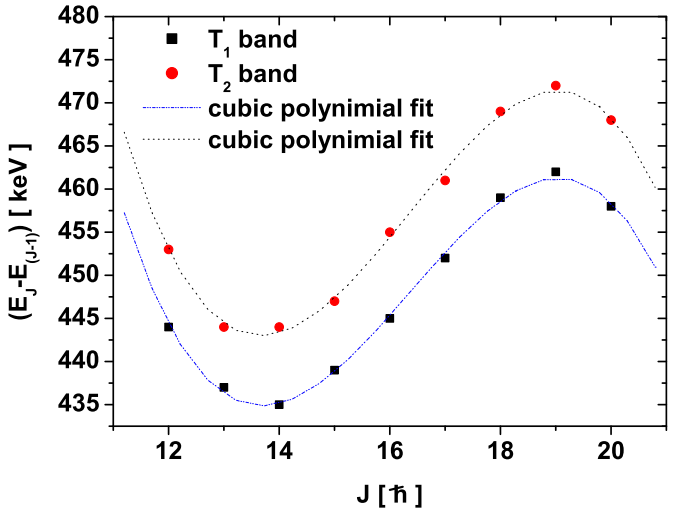

FIG. 3: Energy spacings in the two twin bands T_1 and T_2.

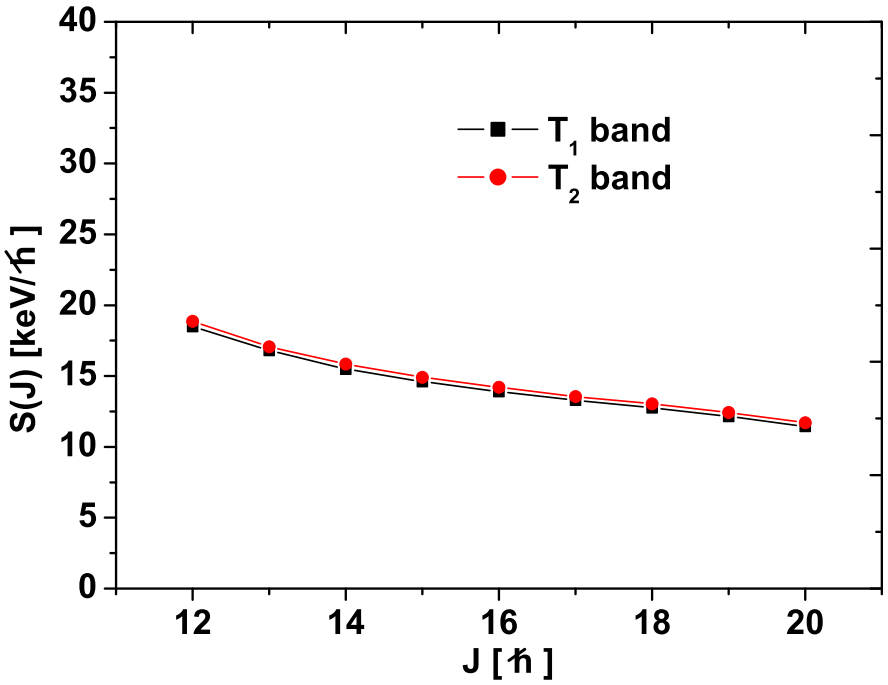

FIG. 4: The signature energy staggering $S(J)$, defined by Eq. (**??**), is represented as function of the angular momentum J, in the bands T_1 and T_2.

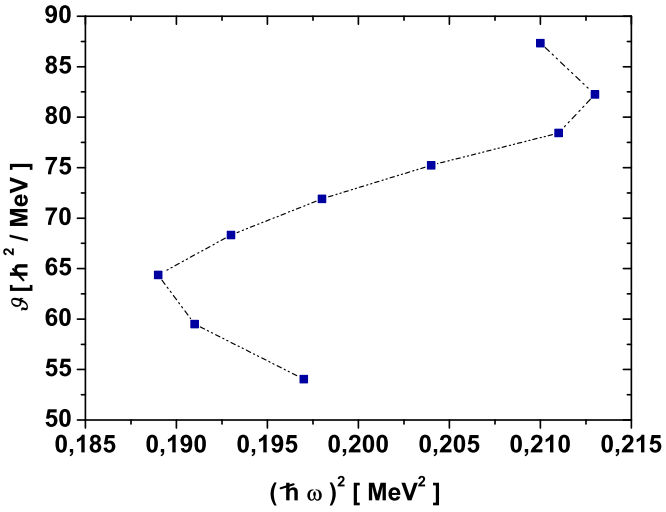

FIG. 5: The double moment of inertia calculated for the angular momenta $12^+ - 20^+$ with Eq.(1.7) are represented as function of the corresponding rotational frequency given by (1.8).

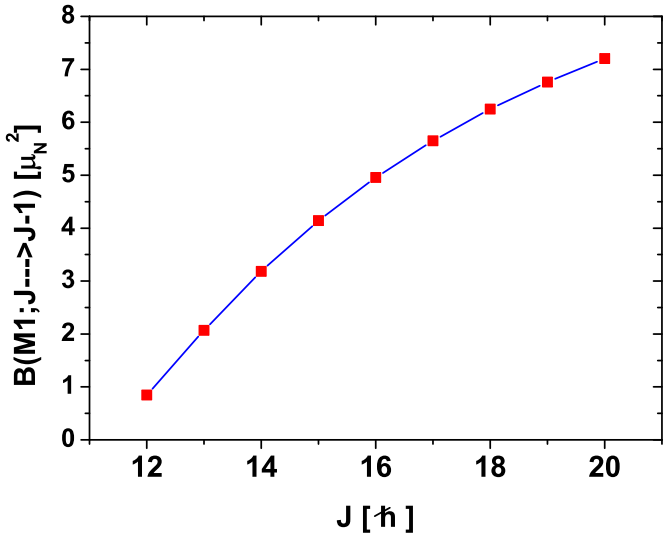

FIG. 6: The $B(M1)$ values associated with the dipole magnetic transitions between two consecutive energy levels, in the T_1 band. The gyromagnetic factors employed in our calculations are: $\mu_p = 0.666\mu_N$, $\mu_n = 0.133\mu_N$ and $\mu_F = 1.289\mu_N$. As usual the spin gyromagnetic factor was quenched by a factor 0.75 in order to account for the influence of the proton excited states on the magnetic moment.

Energies of the bands 1^+ and $\tilde{1}^+$ are free of any adjustable parameters and are presented in Fig.2. In the upper panels two bands of two quasiparticles nature are predicted. These two bands exhibit the properties of a chiral band: a) the energy spacing is almost constant with a slight fluctuation at the begin and end of the interval(see Fig. 3); b) The signature of the energy clustering is defined by the equation:

$$S(J) = \frac{E(J) - E(J-1)}{2J}. \tag{1.6}$$

As shown in Fig. 4 this is almost independent of angular momentum. The moment of inertia characterizing the twin bands plotted as function of the rotational frequency squared, exhibits the back-bending phenomenon.

$$\mathcal{J} = \frac{2(J+1)}{E(J+1) - E(J)}, \tag{1.7}$$

$$\hbar\omega = E(J+1) - E(J). \tag{1.8}$$

The reduced transition probability B(M1) inside the band is large, reaching the value of $7\mu_N^2$ for high spin. The proposed formalism predicts the existence of four twin magnetic bands from which only two were commented here. We consider that our approach contains original hypothesis and will stimulate the experimentalists to extend their measurements to the even-even nuclei.

---

[1] N. Lo Iudice and F. Palumbo, Phys. Rev. Lett. **41**, 1532 (1978).

[2] G. De Francheschi, F. Palumbo and N. Lo Iudice, Phys. Rev. **C29** (1984) 1496.

[3] N. Lo Iudice, Phys. Part. Nucl. **25** , 556, (1997).

[4] D. Zawischa, J. Phys. G**24**, 683,(1998).

[5] S. Frauendorf, Rev. Mod. Phys. **73** (2001) 463.

[6] Jenkins et al., Phys. Rev. Lett. **83** (1999) 500.

[7] A. A. Raduta, A. Faessler and V. Ceausescu, Phys. Rev. **C36** (1987) 2111.

[8] A. A. Raduta, I. I. Ursu and D. S. Delion, Nucl. Phys. **A 475** (1987) 439.

[9] A. A. Raduta and D. S. Delion, Nucl. Phys. **A 491** (1989) 24.

[10] N. Lo Iudice, A. A. Raduta and D. S. Delion, Phys. Lett. **B 300** (1993) 195; Phys. Rev. **C 50** (1994) 127.

[11] A. A. Raduta, D.S. Delion and N. Lo Iudice, Nucl. Phys. **A564** (1993) 185.

[12] A. A. Raduta, I. I. Ursu and Amand Faessler, Nucl. Phys. **A 489** (1988) 20.

[13] A. A. Raduta, A. Escuderos and E. Moya de Guerra, Phys. Rev. **C 65** (2002) 0243121.

[14] A. A. Raduta, N. Lo Iudice and I. I. Ursu, Nucl. Phys. **584** (1995) 84.

[15] A. A. Raduta, Phys. Rev C **A51** (1995) 2973.

[16] A. Aroua, *et al*, Nucl. Phys. **A728** (2003) 96.

[17] A. A. Raduta, C.M. Raduta and Amand Faessler, Phys. Lett. B, 635 (2006) 80.

[18] A. A. Raduta, Al. H. Raduta and C. M. Raduta, Phys. Rev. C74 (2006) 044312.

[19] Raduta et al., Phys. Rev. C 80, 044327 (2009).

[20] A. A. Raduta, V. Ceausescu, A. Gheorghe and R. Dreizler, Phys. Lett. **B 121**1; Nucl. Phys. **A 381** (1982) 253.

[21] A. A. Raduta, A. Faessler and V. Ceausescu, Phys. Rev. **C 36** (1987) 439.

[22] A. A. Raduta, I. I. Ursu and D. S. Delion, Nucl. Phys. **A 475** (1987) 439.

[23] A. A. Raduta and D. S. Delion, Nucl. Phys. **A 491** (1989) 24.

[24] N. Lo Iudice, A. A. Raduta and D. S. Delion, Phys. Rev. **C50** (1994) 127.

[25] A. A. Raduta, C. lima and Amand Faessler, Z. Phys. A - Atoms and Nuclei **313**, (1983), 69.

[26] Coral M. Baglin, Nuclear Data Sheets 113 (2012) 1871.

2. Description of the isotope chain $^{180-196}$Pt within some solvable approaches, A. A. Raduta and P. Buganu, Physical Review C. Phys. Rev. C 88 (2013) 064328.

Once the hypothesis of a specific symmetry for each critical point of a phase transition [1–4] was advanced, many groups investigated both experimentally and theoretically which are the critical nuclei in a isotopic chain. While in the beginning, candidates for the symmetry X(5) [2] have been found in the region of $A \approx 150$ [5–7] recently a new proposal was made for the isotopes of Pt and Os [8, 9]. In Refs. [10, 11], the experimental data for ^{176,178,180,188,190,192}Os have been realistically described using alternatively the approximations of sextic and spheroidal (SSA) [10], Davidson and spheroidal (DSA) [11], infinite square well and spheroidal (ISWSA) [12]. The results were compared with those obtained with the coherent state model (CSM) [13] and X(5 model respectively. According to this study, among these isotopes there are some (^{176}Os and ^{188}Os) exhibiting the specific properties for the critical point in the transition $U(5) \rightarrow Su(3)$. On the other hand, the approximation

sextic and Mathieu (SMA) [14], applied to the isotopes ^{188,190,192}Os leads to the conclusion that ^{192}Os is a candidate for the critical point of the shape transition from oblate to prolate which goes though the triaxial shape with $\gamma_0 = 30^0$.

Encouraged by the results obtained for Os isotopes, the above mentioned approaches have been applied also to $^{180-196}$Pt. In addition to the calculations concerning the excitation energies in the ground, β and γ bands and the intraband as well as the intraband E2 transitions, we also analyzed the shape evolution in the three bands when we pass from one isotope to another. We addressed also the question whether there are signatures for a shape coexistence or a transition from prolate to oblate shape. Here we used a new approximation called Infinite square well and Mathieu (ISWMA) which seems to be appropriate for the triaxial nuclei description.

To achieve the mentioned objectives the paper was structured as follows. First the formalisms used for the quantitative description of the Pt isotopes were briefly reviewed. The numerical results are compared with the corresponding experimental data. Finally the main conclusions are summarized.

In Tables II and III the energies and E2 transition rates determined for ^{180,188,190}Pt by using the formalisms SSA, ISWSA, X(5), SMA, ISWMA and Z(5) are listed. The comparison with the experimental data shows a good agreement.

TABLE II: Spectra for the ground, β and γ bands in ^{180,188}Pt and ^{190}Pt yielded by the SSA, ISWSA, X(5), SMA, ISWMA, Z(5) formalisms respectively, are compared with the experimental data taken from Refs. [15–17].

E [keV]	^{180}Pt				^{188}Pt			^{190}Pt			
J^+_{band}	Exp.	SSA	ISWSA	X(5)	Exp.	SSA	ISWSA	Exp.	SMA	ISWMA	Z(5)
2^+_g	153	126	125	133	266	232	183	296	225	282	284
4^+_g	411	386	366	387	671	645	545	737	645	721	667
6^+_g	757	749	693	724	1185	1170	1045	1288	1206	1259	1130
8^+_g	1182	1194	1093	1131	1783	1772	1667	1915	1872	1885	1668
10^+_g	1674	1705	1563	1604	2438	2429	2405	2535	2620	2591	2276
0^+_β	478	590	649	753	799	719	849	921	832	661	1110
2^+_β	861	809	863	993	1115	1193	1153	1203	1260	1173	1617
4^+_β	1248	1173	1258	1425		1802	1716		1875	1931	2259
6^+_β	1650	1632	1760	1967		2493	2446		2607	2815	2999
8^+_β		2164	2348	2593		3240	3314		3426	3803	3822
10^+_β		2755	3013	3292		4028	4308			4885	4724
2^+_γ	677	840	858	856	606	681	723	598	648	581	521
3^+_γ	963	954	969	971	936	860	887	917	848	812	737
4^+_γ	1049	1101	1105	1110	1085	1098	1089	1128	1159	1183	1254
5^+_γ	1315	1258	1263	1269		1316	1325	1450	1369	1391	1315
6^+_γ		1464	1440	1447	1636	1630	1594	1733	1808	1882	2004
7^+_γ	1727	1653	1637	1642		1868	1893		2009	2062	1949
8^+_γ		1909	1853	1854	2247	2241	2223		2559	2665	2799
9^+_γ	2198	2122	2087	2082		2489	2583		2742	2816	2644
10^+_γ		2421	2338	2326		2911	2971		3391	3222	3647
r.m.s. [keV]		67	92	140		47	81		71	98	206

TABLE III: The reduced E2 transition probabilities yielded by SSA, ISWSA, X(5), and SMA, ISWMA, Z(5) for the isotopes ^{180,188,190}Pt respectively are compared with the experimental data taken from [16–18].

B(E2) [W.u.]	^{180}Pt				^{188}Pt			^{190}Pt			
$J^+_{band} \rightarrow J'^+_{band}$	Exp.	SSA	ISWSA	X(5)	Exp.	SSA	ISWSA	Exp.	SMA	ISWMA	Z(5)
$2^+_g \rightarrow 0^+_g$	153^{+15}_{-15}	110	106	106	82^{+15}_{-15}	82	82	56^{+3}_{-3}	56	56	56
$4^+_g \rightarrow 2^+_g$	140^{+30}_{-30}	168	169	169		136	131		86	95	89
$6^+_g \rightarrow 4^+_g$	≥ 50	202	210	210		171	162		119	138	123
$8^+_g \rightarrow 6^+_g$		230	241	241		200	186		144	169	148
$10^+_g \rightarrow 8^+_g$		255	265	266		226	205		166	191	166

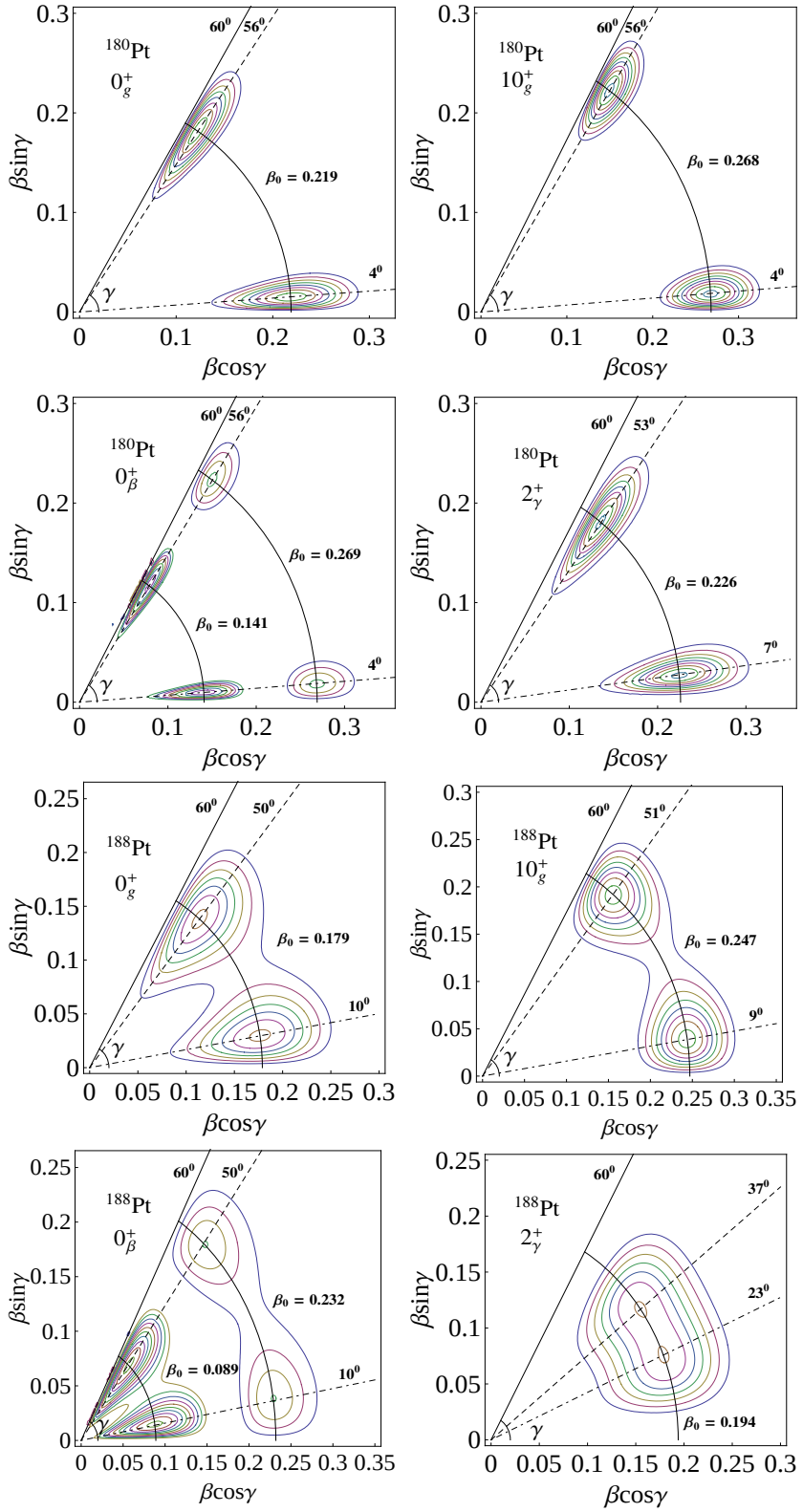

FIG. 7: Probability densities for the states 0^+_g, 10^+_g, 0_β and 2^+_γ in the isotopes ^{180,188}Pt were determined with SSA.

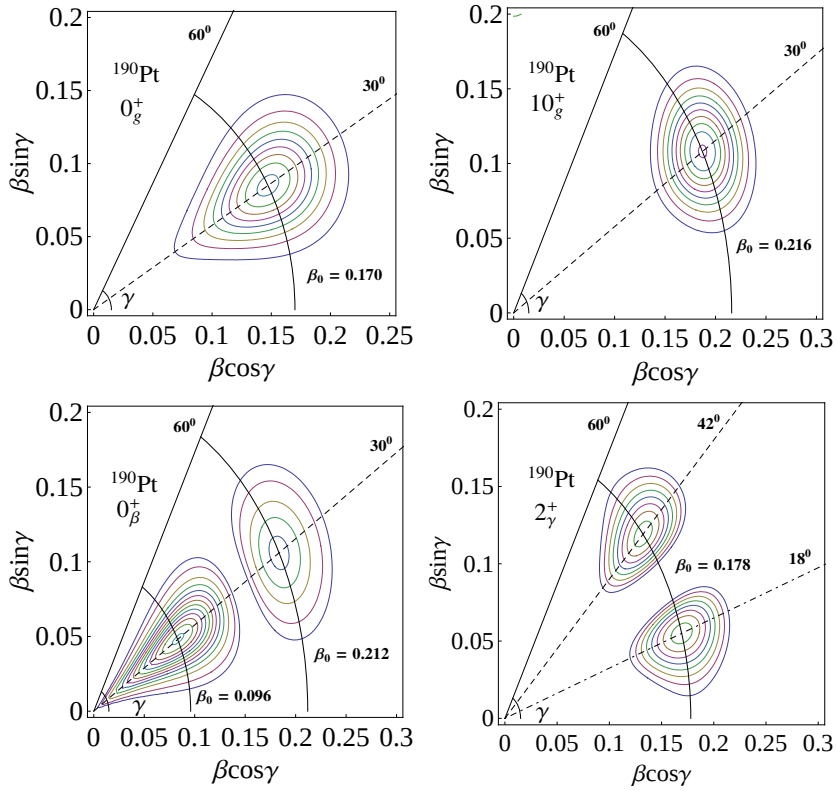

FIG. 8: Probability densities for the states 0^+_g, 10^+_g, 0_β and 2^+_γ in the isotopes ^{190}Pt were determined with SSA.

In Figs. 7 and 8, sections of the probability density and the elementary volume product, for the states 0^+_g, 10^+_g, 0^+_β, 2^+_γ, are given. One notices that the maxima of the γ wave functions squared are reached for $\gamma_0 = 0^0$ and $\gamma_0 = 30^0$. We see that a node in the *beta* functions leads to the existence of two maxima in β for the same value of γ. For ^{188}Pt the equidensity curves surround two maxima for a single value of β. This picture suggests a two shapes coexistence.

In conclusion, we described the energy spectra of ground, β and γ bands as well as the intraband and interband transition probabilities for the chain $^{180-196}$Pt, using several phenomenological models emerging from the liquid drop model. A new approach called ISWMA was proposed, which seems to be suitable for the description of the triaxial nuclei.

[1] F. Iachello, Phys. Rev. Lett. **85** (2000) 3580.

[2] F. Iachello, Phys. Rev. Lett. **87** (2001) 052502.

[3] F. Iachello, Phys. Rev. Lett. **91** 132502 (2003).

[4] D. Bonatsos, D. Lenis, D. Petrellis, P.A. TerzievPhys. Lett. B **588**, 172 (2004).

[5] R. F. Casten and N. V. Zamfir, Phys. Rev. Lett. **87**, 052503 (2001).

[6] R. Krücken *et al.*, Phys. Rev. Lett. **88**, 232501 (2002).

[7] D. Tonev *et al.*, Phys. Rev. C **69**, 034334 (2002).

[8] A. Dewald *et al.*, J. Phys. G: Nucl. Part. Phys. **31**, S1427 (2005).

[9] P. Petkov *et al.*, J. Phys.: Conf. Ser. **366**, 012036 (2012).

[10] A. A. Raduta and P. Buganu, J. Phys. G: Nucl. Part. Phys. **40**, 025108 (2013).

[11] A. A. Raduta, A. C. Gheorghe, P. Buganu and A. Faessler, Nucl. Phys. A **819**, 46-78 (2009).

[12] A. Gheorghe, A. A. Raduta and A. Faessler, Phys. Lett. B **648**, 171 (2007).

[13] A. A. Raduta, V. Ceausescu, A. Gheorghe and R. M. Dreizler, Nucl. Phys. A **381**, 253 (1982).

[14] A. A. Raduta and P. Buganu, Phys. Rev. C **83**, 034313 (2011).

[15] S. -c. Wu and H. Niu, Nuclear Data Sheets **100**, 483 (2003).

[16] Balraj Singh, Nuclear Data Sheets **95** , 387 (2002).

[17] Balraj Singh, Nuclear Data Sheets **99**, 275 (2003).

[18] J. C. Walpe *et al.*, Phys. Rev. C **85** 057302 (2012).

[19] A. Bohr, Mat. Fys. Medd. Dan. Vid. Selsk. **26** (1952) no.14; A.Bohr and B.Mottelson, Mat. Fys. Medd. Dan. Vid. Selsk. **27** (1953) no. 16.

RESULTS, 2014

Stage 4:Chiral symmetry; backbending

I. Deformation properties of the projected spherical single particle basis, A.A. Raduta, R. Budaca, Annals of Physics 347 (2014) 141169.

Deformed single particle energies obtained by averaging a particle-core Hamiltonian with a projected spherical basis depend on a deformation parameter and an arbitrary constant defining the canonical transformation relating the collective quadrupole coordinates and momenta with the boson operators. When the mentioned basis describes the single particle motion of either protons or neutrons the parameters involved are isospin dependent. An algorithm for fixing these parameters is formulated and then applied for 194 isotopes covering

a good part of the nuclide chart. Relation with the Nilsson deformed basis is pointed out in terms of deformation dependence of the corresponding single particle energies as well as of the nucleon densities and their symmetries. The proposed projected spherical basis provides an efficient tool for the description of spherical and deformed nuclei in a unified fashion.

In this paper we exploited the property of the coherent state of being a basis generating function. We were inspired by the paper of Nilsson [1] which defines a deformed wave function as an eigenstate of a Hamiltonian which contains a quadrupole mean field term. Such basis has been used by many authors for the description of the deformed nuclei. However when we want de describe an observable which is very sensitive to the variation of the angular momentum the many body wave function is to be projected over the angular momentum. This operation is not simple at all, for example for the ground state corresponding to the RPA (random phase approximation) only approximate solutions are known so far. In this context any contribution to this field is welcome. In this paper we present a solution for this problem [2, 5–7].

To describe a particle-core interacting system we shall consider the following Hamiltonian

$$\tilde{H} = H_{sm} + H_{core} - M\omega_0^2 r^2 \sum_{\lambda=0,2} \sum_{-\lambda\leq\mu\leq\lambda} \alpha^*_{\lambda\mu} Y_{\lambda\mu}. \tag{1.1}$$

where

$$H_{core} = \omega_b \sum_{\mu} b^\dagger_{2\mu} b_{2\mu} \tag{1.2}$$

is a harmonic quadrupole boson Hamiltonian associated with the phenomenological core. The spherical shell model single-particle Hamiltonian is denoted by H_{SM} The particle-core interaction represented by the last term, depends on the nuclear deformation through the monopole and quadrupole shape coordinates, α_{00} and $\alpha_{2\mu}$. The latter ones are related to the boson operators $b^\dagger_{2\mu}$ defining the harmonic oscillation of the core, through a canonical transformation. The restriction of volume conservation provides a relation between the monopole and quadrupole coordinates:

$$\alpha_{00} = -\frac{1}{2k^2\sqrt{\pi}} \left[5 + \sum_{\mu} \left(2b^\dagger_\mu b_\mu + (b^\dagger_\mu b^\dagger_{-\mu} + b_{-\mu} b_\mu)(-)^\mu \right) \right]. \tag{1.3}$$

Averaging H_{pc} with the eigenstates $|nljm\rangle$ of H_{SM}, one obtains a deformed boson Hamiltonian whose ground state is described by a coherent state:

$$\psi_g = e^{d\left(b_{20}^{\dagger} - b_{20}\right)}|0\rangle_b, \tag{1.4}$$

where $|0\rangle_b$ is the vacuum state of the boson operators, while d is a real parameter which simulates the nuclear deformation. On the other hand, the average of H_{pc} with ψ_g is a single particle Hamiltonian, similar to that of the Nilsson model [1]:

$$H_{mf} = \langle\psi_g|H_{pc}|\psi_g\rangle = \omega_b d^2 + H_{sm} - \hbar\omega_0 r'^2\left[\frac{\sqrt{2}d}{k}Y_{20} - \frac{1}{8\pi k^2}(5+4d^2)\right], \tag{1.5}$$

where the stretched coordinates are used. Further, extracting from the above Hamiltonian the zero point deformation energy

$$\lim_{d\to 0}\left(H_{mf} - H_{SM}\right) = \frac{5\hbar\omega_0 r'^2}{8\pi k^2}, \tag{1.6}$$

one arrives at a more recognizable form:

$$H_{mf} = \omega_b d^2 + H_{SM} - \hbar\omega_0 r'^2\left(\frac{\sqrt{2}d}{k}Y_{20} - \frac{1}{2\pi k^2}d^2\right). \tag{1.7}$$

We note that the deformed terms involved in the Nilsson model Hamiltonian and the mean field H_{mf} are identical provided the following equation holds:

$$\frac{d}{k} = \frac{\beta}{\sqrt{2}}. \tag{1.8}$$

One recovers the original Nilsson Hamiltonian [1]:

$$H_{Nilsson}(\beta) = H_{SM} - \hbar\omega_0 r'^2\beta Y_{20}. \tag{1.9}$$

if in (3.9) one ignores the constant terms i.e., those which are independent of the particle coordinates.

Our proposal [5] was to treat the particle-core system, which is rotationally invariant, with the projected states:

$$\Phi_{nlj}^{IM}(d) = \mathcal{N}_{nlj}^{I}(d)P_{MI}^{I}[|nljI\rangle\psi_g]. \tag{1.10}$$

The tensorial form of this state,

$$\Phi_{nlj}^{IM}(d) = \mathcal{N}_{nlj}^{I}(d)\sum_{J} C_{I\,0\,I}^{j\;J\;I}(N_J^g)^{-1}\left[|nlj\rangle\phi_J^g\right]_{IM}, \tag{1.11}$$

The norm of this state is:

$$(\mathcal{N}^I_{nlj}(d))^{-2} = \sum_J \left(C^{j\ J\ I}_{I\ 0\ I} \right)^2 (N^g_J)^{-2}\,. \tag{1.12}$$

The main properties of the projected states are: a) They are orthogonal with respect to the quantum numbers I and M; b) Although these states belong to the space of particle-core states, they can be used as a single particle basis. Indeed, whenever we want to calculate a matrix element for a one body operator we integrate first over the collective degrees of freedom, the final result being written in a factorize form: one factor contains the dependence on the nuclear deformation while the second one is the matrix element corresponding to the spherical shell model single particle states. To give an example, we consider a many body tensor operator, T^k_μ, of rank k and projection μ. The final result for the matrix elements between two projected spherical states is:

$$\begin{aligned} \langle \Phi^I_{nlj} || T^k || \Phi^{I'}_{n'l'j'} \rangle &= f^{n'l'j'I'}_{nljI}(d) \langle nlj || T^k || n'l'j' \rangle, \quad \text{with} \\ f^{n'l'j'I'}_{nljI}(d) &= \mathcal{N}^I_{nlj}(d) \mathcal{N}^{I'}_{n'l'j'}(d) \hat{j}\hat{I}' \sum_J C^{j\ J\ I}_{I\ 0\ I} C^{j'\ J\ I'}_{I'\ 0\ I'} W(jkJI'; j'I)\, (N^g_J)^{-2}\,; \end{aligned} \tag{1.13}$$

c) The connection between the deformation parameter d, involved in the definition of the coherent state ψ_g, and the nuclear deformation is readily obtained requiring that the deformation terms from the model Hamiltonian and Nilsson Hamiltonian have equal strengths:

$$\frac{d}{k} = \sqrt{\frac{2\pi}{45}} (\Omega^2_\perp - \Omega^2_z). \tag{1.14}$$

Here $\Omega_\perp$ and Ω_z denote the mean field frequencies from the Nilsson model which are related to $\delta = \sqrt{45/16\pi}\beta$ by:

$$\Omega_\perp = (\frac{2+\delta}{2-\delta})^{1/3},\ \Omega_z = (\frac{2+\delta}{2-\delta})^{-2/3}. \tag{1.15}$$

Averaging the particle-core Hamiltonian with the projected state one gets the expression:

$$\begin{aligned} \epsilon^I_{nlj} &= \langle \Phi^{IM}_{nlj}(d) | H' | \Phi^{IM}_{nlj}(d) \rangle = \epsilon_{nlj} - \hbar\omega_0 (N + \frac{3}{2}) C^{j2j}_{I0I} C^{j2j}_{1/201/2} \frac{(\Omega^2_\perp - \Omega^2_z)}{3} \\ &+ \hbar\omega_0 (N + \frac{3}{2}) \left[1 + \frac{5}{2d^2} + \frac{\sum_J (C^{jIJ}_{I-I0})^2 I^{(1)}_J}{\sum_J (C^{jIJ}_{I-I0})^2 I^{(0)}_J} \right] \frac{(\Omega^2_\perp - \Omega^2_z)}{90}. \end{aligned} \tag{1.16}$$

Here the standard notation for the Clebsch Gordan coefficients have been used, $C^{j_1 j_1 j}_{m_1 m_2 m}$. The overlap integrals $I^{(k)}_J$ have been analytically studied in some previous publications. If

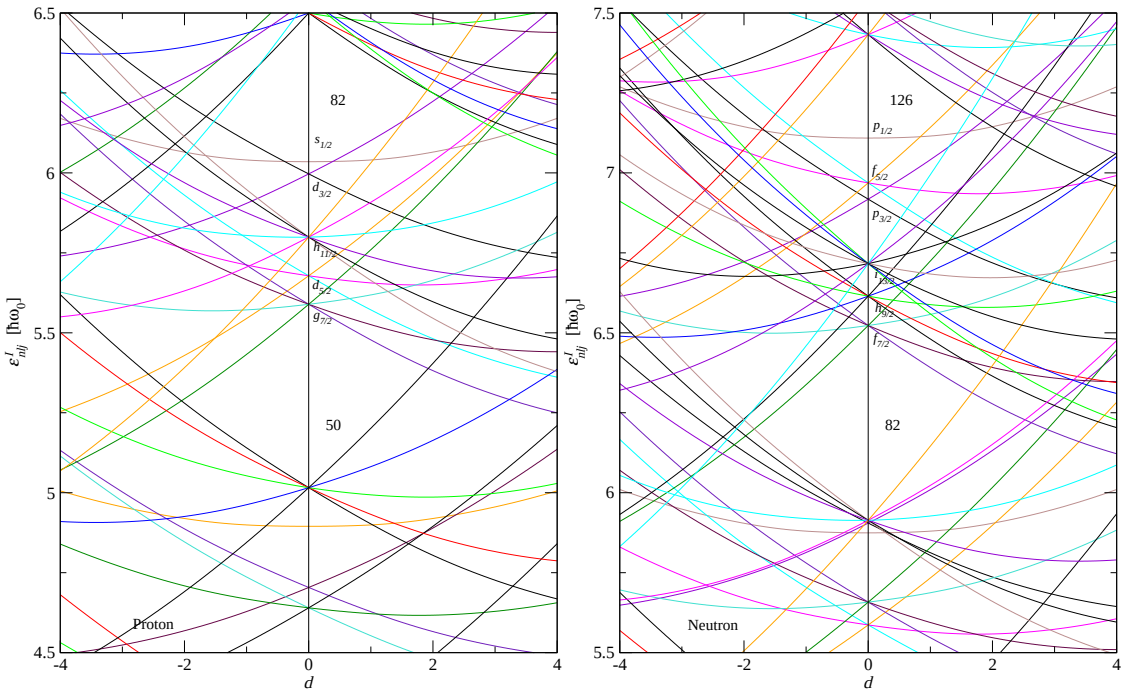

FIG. 9: Proton and neutron single-particle energies in the region of $N = 5$ and $N = 6$ shells respectively, given by Eq.(1.17) where the shell model parameters $\kappa = 0.0637$ and $\mu = 0.60$ for protons and $\mu = 0.42$ for neutrons were used. The canonical transformation constant is fixed to $k = 10$.

from the above expression one subtract the zero point energy contribution one obtains the final expression for the single particle energies, specific to the proposed model.

$$\begin{aligned}\epsilon^I_{nlj} &= = \epsilon_{nlj} - \hbar\omega_0(N+\frac{3}{2})C^{j2j}_{I0I}C^{j2j}_{1/201/2}\frac{(\Omega^2_\perp - \Omega^2_z)}{3} \\ &+ \hbar\omega_0(N+\frac{3}{2})\left[1+\frac{\sum_J (C^{jIJ}_{I-I0})^2 I^{(1)}_J}{\sum_J (C^{jIJ}_{I-I0})^2 I^{(0)}_J}\right]\frac{(\Omega^2_\perp - \Omega^2_z)}{90} \\ &-\hbar\omega_0\left(N+\frac{3}{2}\right)\left[j-I+\frac{1}{2}\left(1-(-)^{j-I}\right)\right]\frac{1}{8\pi k^2}. \end{aligned} \tag{1.17}$$

The averages (1.17) can be viewed as approximations of the single-particle energies in the deformed Nilsson orbits. As a matter of fact these are very close to the single-particle energies (**??**) of the projected Nilsson states obtained by diagonalization within a single major shell ($\Delta N = 0$). This is illustrated in Fig. 9.

Notice that although the single particle energies of our model are similar with the Nilsson model energies, the states degeneracies are different. To make the wave functions of the two models compatible we change the norm of the projected single particle state to:

$$\langle \Phi_\alpha^{IM} | \Phi_\alpha^{IM} \rangle = 1 \Longrightarrow \sum_M \langle \Phi_\alpha^{IM} | \Phi_\alpha^{IM} \rangle = 2. \tag{1.18}$$

Due to this normalization, on each state I with 2I+1 sub-states one could distribute at most 2 nucleons. The notation α was used for the set of shell model quantum numbers $|nljm\rangle$.

A. Nucleon density

The density operator corresponding to the projected spherical states can be written as:

$$\hat{\rho} = \sum_{nljIM} \frac{2}{2I+1} \left| \Phi_{nlj}^{IM}(d) \right|^2 . \tag{1.19}$$

Using the tensorial form of the projected particle-core state (1.11), and replacing the product of the projected core states and their corresponding complex conjugates by their scalar product, one obtains:

$$\langle \hat{\rho} \rangle_{coll} = 2 \sum_{nljm>0} \left| |nljm\rangle \right|^2 , \tag{1.20}$$

which is exactly the spherical shell model nucleon density. The consistency with the projected Nilsson states is then complete.

However, it is desirable to induce a deformation dependence of the particles distribution. Inspired by the fact that the deformation dependence of the mean field is obtained by averaging the particle-core Hamiltonian with the quadrupole boson coherent state (1.4), we extend the procedure to the nucleon density (1.19) with the results:

$$\langle \psi_g | \hat{\rho} | \psi_g \rangle = \sum_{nljIM} \frac{2}{2I+1} \left| \langle \psi_g | \Phi_{nlj}^{IM}(d) \rangle \right|^2 . \tag{1.21}$$

Similarly, the wave function associated to the deformed mean filed can be looked at as the overlap of the projected spherical state and the coherent state describing the core.

$$\langle \psi_g | \Phi_{nlj}^{IM}(d) \rangle = \mathcal{N}_j^I \sum_J F_{JM}^{jI}(d) | nljM \rangle, \tag{1.22}$$

where

$$F^{jI}_{JM}(d) = C^{j\,J\,I}_{I\,0\,I} C^{j\,J\,I}_{M\,0\,M} (N_J)^{-2}\,. \tag{1.23}$$

A direct connection between the k-pole transition densities defined by the projected spherical single particle and the spherical shell model bases, can be obtained by using the second quantization form of a one body operator, which is a tensor of rank k and projection m with respect to the rotation transformations:

$$\begin{aligned}
\hat{T}_{km} &= \sum \sqrt{\frac{2}{2I+1}} \langle \Phi^{IM}_{nlj} | \hat{T}_{km} | \Phi^{I'M'}_{n'l'j'} \rangle \sqrt{\frac{2}{2I'+1}} c^{\dagger}_{\alpha IM} c_{\alpha' I' M'} \\
&= \sum \frac{2}{\hat{I}\hat{I}'} \langle \Phi^{I}_{nlj} || \hat{T}_k || \Phi^{I'}_{n'l'j'} \rangle C^{I'kI}_{M'mM} c^{\dagger}_{\alpha IM} c_{\alpha' I' M'} \\
&= \sum_{\alpha I;\alpha' I'} \frac{2}{\hat{I}\hat{I}'} \langle \alpha I || \hat{T}_k || \alpha' I' \rangle \hat{\rho}^{ps}_{km}(\alpha I; \alpha' I').
\end{aligned} \tag{1.24}$$

For the sake of simplicity we used the abbreviations:

$$\begin{aligned}
|\alpha IM\rangle &= |\Phi^{IM}_{nlj}\rangle, \;\; \alpha = (nlj), \; \hat{I} = \sqrt{2I+1}, \\
\hat{\rho}^{ps}_{km}(\alpha I; \alpha' I') &= -\frac{\hat{I}}{\hat{k}} \left(c^{\dagger}_{\alpha I} c_{\widetilde{\alpha' I'}} \right)_{km}, \;\; c_{\widetilde{\alpha IM}} = (-1)^{I-M} c_{\alpha I,-M}.
\end{aligned} \tag{1.25}$$

The index "ps" suggests that the density matrix is associated to a projected spherical basis. As for the shell model we have:

$$\begin{aligned}
\hat{T}_{km} &= \sum \langle nlj || \hat{T}_k || n'l'j' \rangle \hat{\rho}^{sm}_{km}(nlj; n'l'j'), \text{ with} \\
\hat{\rho}^{sm}_{km}(nlj; n'l'j') &= -\frac{\hat{j}}{\hat{k}} \left(c^{\dagger}_{nlj} c_{\widetilde{n'l'j'}} \right)_{km}.
\end{aligned} \tag{1.26}$$

Using the relationship of the matrix elements corresponding to the two bases we have:

$$\hat{\rho}^{sm}_{km}(nlj; n'l'j') = \sum_{I,I'} \frac{2}{\hat{I}\hat{I}'} f^{j'I'}_{jI;k(d)} \hat{\rho}^{ps}_{km}(nljI; n'l'j'I'). \tag{1.27}$$

Taking into account the explicit expression of the norms $\mathcal{N}^I_j$ and the analytical form of the Racah coefficient with one vanishing index, it can be proved that for $k = 0$ the factor f is equal to unity:

$$f^{j'I'}_{jI;0}(d) = \delta_{I,I'} \delta_{j,j'}. \tag{1.28}$$

Consequently one obtains:

$$\hat{\rho}^{sm}_{00}(nlj; nlj) = \sum_{I} \frac{2}{2I+1} \hat{\rho}^{ps}_{00}(nljI; nljI). \tag{1.29}$$

Going back to the definition of $\hat{\rho}$ in the two basis, (3.30) and (3.31), by a direct and simple calculation one finds that Eqs. (1.29) and (3.24) are identical.

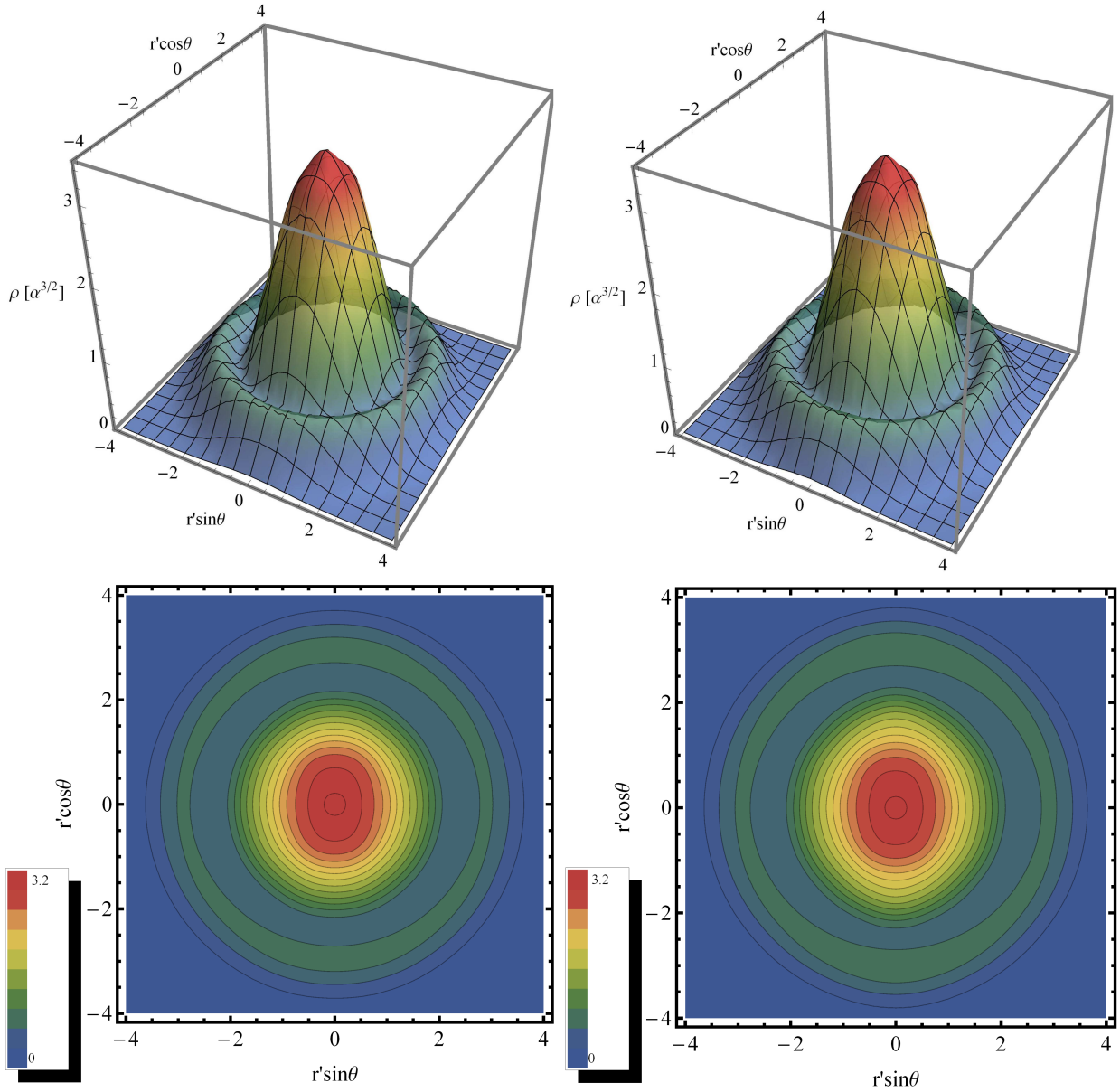

FIG. 10: Total nuclear density given by Eq.(1.20) is represented as function of $x = r' \sin\theta$ and $z = r' \cos\theta$ in units of $\alpha^{\frac{3}{2}}$ in 3D plots (up) and contour plots (down) for ^{150}Gd (left) and ^{156}Gd (right). In both cases the densities corresponding to two adjacent curves differ from each other by $0.21\alpha^{3/2}$.

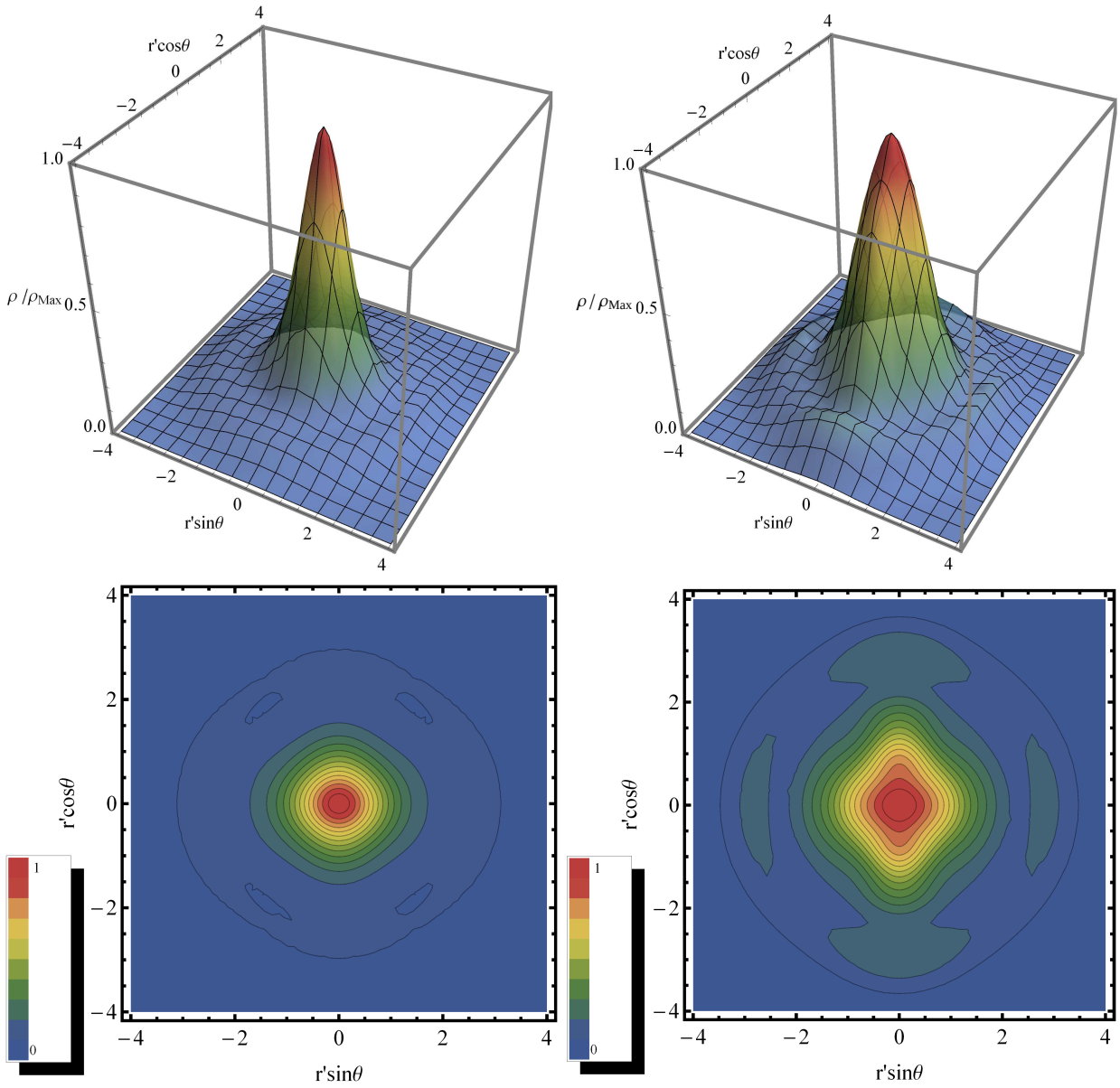

FIG. 11: Total nuclear density projected on the quadrupole boson coherent state defined by Eq.(1.20) and normalized to its maximum value is represented as function of $x = r' \sin\theta$ and $z = r' \cos\theta$ in 3D plots (up) and contour plots (down) for ^{150}Gd (left) and ^{156}Gd (right). Contour plots are made with a step of $0.062/\rho_{max}$.

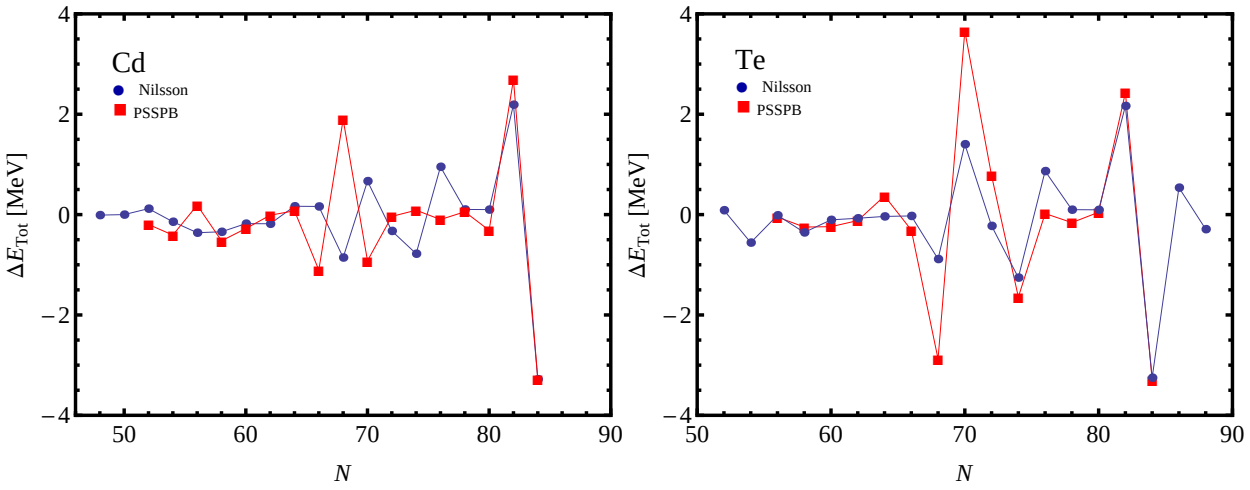

FIG. 12: The binding energy second order difference, ΔE_{Tot} for the isotopes of Cd (left panel) and Te (right panel) is represented as function of the number of neutrons, N. For Nilsson model calculations we included also the ΔN =2 matrix elements with $N_{cutoff} = 10$.

B. Quadrupole moment of the first state 2^+

Let us derive the expression of the quadrupole moment within the GCSM. The liquid drop model (LDM) predicts for the quadrupole moment the expression:

$$Q_{2\mu} = \frac{3ZeR_0^2}{4\pi}\left(\alpha_{2\mu} - \frac{10}{\sqrt{70\pi}}(\alpha_2\alpha_2)_{2\mu}\right), \; R_0 = 1.2A^{1/3}fm. \tag{1.30}$$

Within LDM the state 2^+ is a one phonon state, $b^\dagger_{2\mu}|0\rangle$, which yields for the quadrupole moment, with the standard definition, the expression:

$$\langle 22|Q_{20}|22\rangle = -\frac{3ZeR_0^2\sqrt{5}}{7\pi k^2\sqrt{\pi}}. \tag{1.31}$$

From here it results that for spherical nuclei the quadrupole moment is always negative. The GCSM defines the state 2^+ by the angular momentum projected state $\phi^g_{JM}(d_n, d_p)$ (see Eq. (4.2)) while the quadrupole moment, in the boson representation, is:

$$Q_{20} = \frac{3ZeR_0^2}{4\pi}\left[\frac{1}{k_p\sqrt{2}}\left(b^\dagger_{b0} + b_{p0}\right) - \frac{5}{k_p^2\sqrt{70\pi}}\left((b^\dagger_p b^\dagger_p)_{20} + (b_p b_p)_{20} + (b^\dagger_p b_p)_{20}\right)\right]. \tag{1.32}$$

Averaging this operator with the projected state mentioned above one obtains:

$$\langle\phi^g_{22}(d_n,d_p)|Q_{20}|\phi^g_{22}(d_n,d_p)\rangle = -\frac{3ZeR_0^2}{7\pi}\left[\frac{1}{\sqrt{2}}\frac{d_p}{k_p} + \frac{1}{7}\sqrt{\frac{5}{\pi}}\left(\frac{d_p}{k_p}\right)^2\left(1 + \frac{I^{(1)}_2(\rho)}{I^{(0)}_2(\rho)}\right)\right]. \tag{1.33}$$

This equation might be used to determine the ratio d_p/k_p and then the other parameters, d_n and k_n.

C. Order of shell filling: the magic numbers and the spins of the odd system ground state

Another issue addressed in this paper regards the ability of the proposed model to describe the shell filling and how that compares with what we know from the Nilsson model. To this aim we calculated the second order binding energy difference

$$\Delta E_{Tot} = -\frac{3}{16}\left[2E(N) - E(N+2) - E(N-2)\right], \tag{1.34}$$

with $E(N)$ denoting the total sum of proton and neutron single particle energies for a nucleus with N neutrons. This quantity is plotted for the isotopic chains of Cd and Te in Fig. 8. We notice that both models show two major peaks corresponding to the magic number 82 and the shell filling at $N = 68$ for Cd and $N = 70$ for Te. The distributions of peaks for Te isotones obtained with the projected spherical single particle basis (PSSPB) and Nilsson model respectively, are similar. Some differences appear in the case of Cd's. In the case of Nilsson plot there is a peak for $N = 76$ which is missing in our case. On the other hand the plot with PSSPB exhibits a peak for $N = 56$ which is missing in the case of the plot made with the Nilsson model. The major peak at $N = 70$ for Nilsson model is shifted to $N = 68$ for our method. The order of the shell filling is, of course, depending on the quadrupole deformation. A test for this feature is to identify the levels around the last occupied one and compare their spin with the experimental value for the ground state spin, in an even-odd nucleus. The results are compared with the data for a few odd nuclei in Table XVII. Among the identified angular momenta for the last and the second last occupied as well as for the first unoccupied levels one finds the angular momenta characterizing the ground state according to the experimental data. The reason we listed all three spins is that in the region of the Fermi sea the level density is high and a small uncertainty in determining the deformation may change the position of the level crossing and thus the filling order. Moreover our estimation does not take into consideration the effect of the residual interaction which may also shift the position of the Fermi level. We note that the agreement is reasonable good suggesting that the ground state has the spin of

the first unoccupied level for ^{155}Gd, ^{167}Er, ^{177}Hf, ^{179}Hf and that of the second last occupied state for ^{187}Os, ^{189}Os, ^{157}Gd.

D. Model parameters

Besides the parameters involved in the shell model Hamiltonian there are another two, namely the deformation parameter d and canonicity parameter k. In the case we study isospin depending properties we have to use a set of wave functions, with the parameters d_p and k_p different from those corresponding to the neutrons, denoted by d_n and k_n.

These parameters have been determined according to the following algorithm: a) Equating the theoretical result concerning the energy ratio of the states 4^+ and 2^+ from the ground band, denoted by $R_{4/2}$, with the experimental one, we determine the global deformation parameter ρ $(=d\sqrt{2})$; Inserting this value in Eq.(1.6), one obtains the parameter k; c) From the expression of the reduced transition probability $0_g^+ \to 2_g^+$, one determines k_p; d) Using again Eq. (1.6), but for protons we get d_p; e) From the equation $\rho(=((d_p^2 + d_n^2)^{1/2})$ one determines d_n; f) Then Eq. (1.6) used for neutrons, yields k_n. This procedure has been applied for 194 nuclei and the results collected in several tables. Results for k, k_p and k_n can be interpolated with linear functions of A, the mass atomic number:

$$k = 0.0513471 \cdot A + 4.28957, \;\; rms = 2.59477, \tag{1.35}$$

$$k_p = 0.0488292 \cdot A + 4.61187, \;\; rms = 2.71376, \tag{1.36}$$

$$k_n = 0.0538922 \cdot A + 3.80843, \;\; rms = 3.17185. \tag{1.37}$$

The projected spherical single particle basis has been positively tested by realistically describing the deformed atomic clusters [2], the basic properties of the magnetic dipole mode of scissors type (for Sm isotopes)[6] and by calculating the Gammow-Teller transition amplitude for the double beta decay [7].

To conclude, the coherent state approach is very useful not only for accounting for some phenomenological properties of complex nuclei, but also for providing a unified description

TABLE IV: With the nuclear deformation β taken for Ref.[4] and the deformation parameters as well as the canonicity constants determined as discussed in the text we determined the quantum numbers $[Nljl]$ of the last occupied (Locc), the second last occupied (Slocc) and the first unoccupied (Funocc) neutron states of several even-odd isotopes. Presuming that the Fermi sea is close to one of the mentioned states we can get information upon the spin of the ground state of the odd system whose experimental values (see [3] p. 78) are listed on the last column. Indeed in the region of the last occupied state the level density is high which results that the odd nucleon position is sensitive to the residual interaction.

Nucleus	β_2	ρ	d	k	d_p	k_p	d_n	k_n	Locc	Slocc	Funocc	I_{Exp}
^{155}Gd	0.252	2.939	2.078	12.4534	1.951	11.6878	2.199	13.1745	$[66\frac{13}{2}\frac{1}{2}]$	$[55\frac{9}{2}\frac{3}{2}]$	$[66\frac{13}{2}\frac{3}{2}]$	$\frac{3}{2}$
^{157}Gd	0.271	3.161	2.235	12.5011	2.088	11.6810	2.373	13.2707	$[66\frac{13}{2}\frac{1}{2}]$	$[55\frac{9}{2}\frac{3}{2}]$	$[66\frac{13}{2}\frac{5}{2}]$	$\frac{3}{2}$
^{167}Er	0.294	3.697	2.614	13.5377	2.430	12.5842	2.786	14.4282	$[53\frac{7}{2}\frac{5}{2}]$	$[55\frac{9}{2}\frac{5}{2}]$	$[66\frac{13}{2}\frac{7}{2}]$	$\frac{7}{2}$
^{177}Hf	0.277	3.403	2.406	13.1820	2.245	12.2975	2.557	14.0107	$[53\frac{5}{2}\frac{1}{2}]$	$[51\frac{3}{2}\frac{1}{2}]$	$[55\frac{9}{2}\frac{7}{2}]$	$\frac{7}{2}$
^{179}Hf	0.278	3.415	2.415	13.1845	2.252	12.2973	2.567	14.0157	$[55\frac{9}{2}\frac{7}{2}]$	$[53\frac{5}{2}\frac{1}{2}]$	$[66\frac{13}{2}\frac{9}{2}]$	$\frac{9}{2}$
^{187}Os	0.212	2.588	1.830	12.9232	1.735	12.2539	1.920	13.5595	$[53\frac{7}{2}\frac{7}{2}]$	$[53\frac{5}{2}\frac{1}{2}]$	$[55\frac{9}{2}\frac{9}{2}]$	$\frac{1}{2}$
^{189}Os	0.183	2.234	1.580	12.8377	1.514	12.3051	1.643	13.3491	$[55\frac{9}{2}\frac{9}{2}]$	$[53\frac{5}{2}\frac{1}{2}]$	$[66\frac{13}{2}\frac{11}{2}]$	$\frac{1}{2}$

of spherical and deformed nuclei by means of a projected spherical single particle basis.

---

[1] S. G. Nilsson, Dan. Mat. Fys. Med. **16**, 29 (1955).

[2] A. A. Raduta, E. Garrido and E. Moya de Guerra, Eur. Phys. Jour. **D 15** (2001) 65.

[3] P. Ring and P. Schuck, *The Nuclear Many-body Problem* (Springer Verlag, 1980).

[4] P. Möller, J. R. Nix, W. D. Myers, and W. J. Swyatecki, Atomic Data and Nuclear Data Tables **59**, 185 (1995).

[5] A. A. Raduta, D. S. Delion, and N. Lo Iudice, Nucl. Phys. A **551**, 93 (1993).

[6] A. A. Raduta, A. Escuderos, and E. Moya de Guerra, Phys. Rev. C **65**, 024312 (2002).

[7] A. A. Raduta, and C. M. Raduta, and A. Escuderos, Phys. Rev. C **71**, 0244307 (2005).

II. The SSD hypothesis (single state dominance)

The validity of the SSD hypothesis has been checked for the situation when in describing the $2\nu\beta\beta$ process the gauge invariance is restored. In the literature, three cases of $2\nu\beta\beta$ where the major contribution (over 95%) to the decay rates is brought by a single magnetic dipole state of the intermediate odd-odd system, have been identified. In these cases the first state 1^+ characterizing the odd-odd intermediate nucleus, is either the ground state or a state lying very close to the ground state. For this purpose we used the projected spherical single particle basis described before and a fully renormalized pnQRPA approach with the gauge invariance restored. Our calculations on this line show that under the mentioned circumstances the SSD hypothesis is no longer valid and moreover the Ikeda sum rule is satisfied.

RESULTS, 2015

Stage 5: Specific properties of the chiral magnetic bands

In what follows I shall describe the main results obtained during the year 2015.

I. Nuclear structure with coherent states,Apolodor Aristotel Raduta, Book, 521 pagini, Springer, Heidelberg, New York, London, ISBN 978-3-319-14641-6, DOI 10. 1007/978-3-319-14642-3

The book is very useful for physicists working in the field of nuclear structure

Highlights

Arguments in the favor of coherent state description. Since the coherent state was used for the first time by Glauber for a system of photons, many progresses have been made in extending the concept to other systems with various goals. The ground state properties of a many body system is often described by coherent state as happens within BCS theory, random phase approximation or the time dependent Hartree-Fock (TDHF) formalisms. In general, the dequantization procedure defined by a time dependent variational equation is most reliable when the trial function is of a coherent type. Indeed, only in this case quantizing the classical trajectories the resulting spectrum might be close to that associated with the initial many-body Hamiltonian. Such a treatment can be applied also to quadrupole boson Hamiltonians.

The over-complete property of a coherent state allows for accounts of the dynamics causing the collective motion. Indeed, by expanding the coherent state in a Hilbert space basis, no expansion coefficient is missing. Due to this property, for a quadrupole boson Hamiltonian contributions in the whole boson space are included, which is not the case when a diagonalization procedure is adopted. The useful consequence of the mentioned property is the role of the coherent state as a generating function for a basis of states in the considered Hilbert space.

Here we deal with quadrupole boson Hamiltonians and therefore we use axially symmetric coherent state defined by the quadrupole boson, b^+_{20} and b_{20}, and simple polynomial excitations of that. It is generally accepted that the nuclear system behaves more or less classically in a state of high angular momentum. This fact recommends the coherent states as an efficient tool for treating the high spin states. Indeed, it is well known that the coherent states minimize the Heisenberg uncertainty relations, which in fact reflects a classical character. However, the coherent state breaks several symmetries among which the most important are the rotational and the gauge ones. The question is whether restoring these symmetries, the classical properties are preserved or not. This feature is studied in Phys. Rev. C 86, 054307 for the mentioned symmetries and two pairs of conjugate coordinates: the quadrupole coordinate and its conjugate momentum and the boson number operator

and the conjugate phase.

Studying a second order boson Hamiltonian within a time dependent variational formalism with a quadrupole coherent state as a trial function, and a constraint, the corresponding classical equation is exactly solvable, which results in having a closed formula for the ground band energies, which generalizes the result of Holmberg and Lipas. In the classical picture the kinetic and potential energies are naturally separated. The potential is just the Davidson potential. Alternatively, the energy can be obtained with the angular momentum projected state, i.e. within an approach of variation after projection. An analytical formula for energies, similar to that resulting in a semi-classical treatment, is obtained. The two very simple formulas have been applied to 44 nuclei covering regions characterized by different dynamic symmetries or, in other words, belonging to various known nuclear phases. In all cases one obtains a very good agreement with the experimental data.

The coherent state description. Being encouraged by the results obtained for the ground band, we extended these ideas to three interacting bands, ground, beta and gamma. We started with an axially symmetric coherent state as a model state of the ground band in the intrinsic frame and two polynomial excitations of that, which are associated to the beta and gamma band. The excitations where chosen such that the three states to be orthogonal before and after angular momentum projection. The three sets of projected states have very attractive properties:1) they depend on a real parameter which simulates the nuclear deformation. 2) when the deformation is going to zero the functions for the ground band tend to the highest seniority states $|\frac{J}{2}\frac{J}{2}0JM\rangle$, while those for gamma and beta bands go the the second and third highest seniority states. When the deformation is large the projected wave functions are identical with those provided by the liquid drop model. Moreover, the continuous link between the two sets of wave functions, in vibrational and rotational limits, is the same as the correspondence established empirically by Sheline and Sakai. Within the restricted boson space of projected states we considered an effective boson Hamiltonian, which yields maximally decoupled bands. For a given J the energies for beta band and gamma band states of odd angular momentum are taken to be the corresponding average values while the states of ground band and gamma band of even angular momenta are obtained by diagonalizing a 2x2 matrix. Energies and quadrupole transition probabilities are given in an analytical form, which in the vibrational as well as rotational limits become very simple. This model is called the Coherent State Model (CSM) and has been applied

to a huge number of nuclei belonging to different symmetry regions. Salient features are analytically pointed out within both the laboratory and intrinsic frame.

Several Extension of CSM. The CSM was subject of several extensions: 1) A particle-core Hamiltonian with the core described by the CSM was considered in particle-core space to describe the properties caused by the crossing of the ground, beta and gamma bands with

a two quasiparticle-core band where the particle-like angular momentum is aligned to the collective one leading to several backbendings. The model was applied to the Pt region where several states 12^+ have been seen. In a similar spirit we described the one and three quasiparticle bands in even odd nuclei 2) We attached to the quadrupole bosons an isospin quantum number distinguishing the proton-like from the neuron-like bosons. The formalism obtained following a similar path and arguments as for CSM was conventionally called the Generalized Coherent State Model (GCSM). This new approach describes simultaneously the major bands , ground, beta and gamma, and one band built on the top of the scissors state 1^+. We proved analytically that the GCSM predicts for the total M1 strength, of exciting 1^+ from the ground state 0^+, a quadratic dependence on the nuclear deformation, which in fact confirms the collective character of the mode. Based on a semi-classical calculations we have derived an analytical expression for the gyromagnetic factor of neutrons which corrects the M1 transition operator towards improving the agreement with the data. The GCSM was the first approach which was extended as to describe the scissors modes in the even-odd nuclei, our predictions being later on confirmed by experiment.

3) Recently, the GCSM Hamiltonian was amended by a mean field, a pairing and a particle-core term consisting of a quadrupole-quadrupole and a spin-spin interaction. The collective magnetic dipole band is crossed by four two quasiparticle magnetic bands which have a chiral character. The chiral symmetry is broken by the spin-spin term in four different ways, which results in having four twin bands. I just mention that this is the first formalism which treats the twin bands in even-even nuclei.

4) The CSM may be easily extended to the negative parity states if the unprojected state of ground band is replaced by a product function of two coherent states, one of quadrupole and one of octupole type. In this way the unprojected ground state violates not only the rotational symmetry but also the space reflection symmetry. Therefore, in the laboratory frame we have to restore not only the rotational symmetry but also the parity. In this way, instead of three bands described by the CSM we have three pairs of parity bands. The space

was enlarged by adding two dipole parity partner bands. We kept the principles governing the CSM in constructing the generating functions for independent bands and the effective Hamiltonian. Thus, the extension provides a realistic description of four rotational bands, four of positive and four of negative parity. The properties of these bands have been studied in several publications. Excitation energies of these bands as well as B(E2), B(E1) and B(E3) values have been described for a large number of nuclei.

5) Adding to the Hamiltonian used at 4) an odd particle we extended the description to the odd nuclei. Here we describe realistically six rotational bands, three of positive and three of negative parity bands. One points out that one pair of parity partner bands exhibits a chiral symmetry.

Projected spherical single particle basis Averaging a particle core-Hamiltonian with a coherent state one obtains a deformed mean field which resembles the Nilsson Hamiltonian. On the other hand averaging the particle-core Hamiltonian with the spherical single particle wave function one obtains a boson Hamiltonian which admits the axially deformed quadrupole coherent states as eigenfunctions. This suggest that projecting out the good angular momentum from the product function of a spherical shell model state and an axially deformed quadrupole coherent state might be an efficient basis to treat the particle core-Hamiltonian. From the projected states we succeeded to select a basis. This basis can be used to treat particle-like Hamiltonians. Indeed, when the matrix element of a particle operator is calculated, first the boson factors are orthogonalized leading to a factor depending on nuclear deformation. In particular, the average of the particle-core Hamiltonian with an element of the projected spherical basis gives a set of single particle energies whose deformation dependence is similar to that of Nilsson model states. Moreover, when the deformation is going to zero the single particle energies go to those of spherical shell model. Therefore the defined basis has the nice property that recovers the shell model basis in the vibrational limit, while when the deformation goes apart from zero the Nilsson model energies are obtained. This feature allows us to treat in an unified fashion the spherical and deformed nuclei. This was tested by describing the scissors-like modes and the rate of the $2\nu\beta\beta$ decay. A systematic analysis including 190 nuclei from all regions of the nuclides periodic table, is presented in a very recent paper submitted to Annals of Physics (NY).

A phenomenological solvable model. Starting from the Bohr-Mottelson Hamiltonian written in the intrinsic coordinates supplemented by a specific potential term, by expanding

the rotational and potential terms in series of the variable γ around its static values, 0^0 and 30^0, we obtained a separable form for the differential equations associated to the dynamic deformation variables, which are fully solvable. Thus, the equation in γ is satisfied by the spheroidal or Mathieu functions. Regarding the β variable, the equations used are alternatively those for a sextic oscillator potential with a centrifugal barrier included, an infinite square well or a Davidson potential. Solutions were used to describe the ground, beta and gamma bands energies and E2 transition probabilities for axially deformed and triaxial nuclei, respectively.

Comparison with other models A special chapter is devoted to the comparison of our methods and some phenomenological models which are very popular in the field nuclear structure: a) The liquid drop model b) The deformed liquid drop the model of Greiner and Faessler c) The model of Gneuss and Greiner d) The Interacting Boson Approximation proposed by Arima and Iachello. e) The model of Lipas and Hapakowski f) The methods developed by the group of Bonatsos for interacting rotational bands g) The two rotors model proposed by Lo Iudice and Palumbo h) Nilsson model i) The phenomenological solvable models mentioned above.

The book covers the essential features of a large variety of nuclear structure properties of both collective and microscopic nature. Most of results are given in an analytical form which give a deep insight of the considered phenomena. The detailed comparison with all existent nuclear structure models provides the readers a proper framework and, at a time, the perspective of new developments. The book is very useful for young as well as for experienced researchers. Due to the selfcontent exposure, the book can be successfully read and used also by the undergraduate students.

II. Description of chiral bands in 188;190Os

Rotational spectra appear to be a reflection of the spontaneous rotational symmetry breaking, when the nuclear systems acquires a static deformed shape. Fundamental properties like the nuclear shape, mass and charge density distribution inside nucleus, electric and magnetic moments, collective spectra may be evidenced out by the interaction of the nuclear system with an electromagnetic field. The two components of the field are used to investigate the electric and magnetic properties, respectively. At the end of the last century the magnetic dipole states of scissors type [1, 2] as well as those of spin-flip type [4] have been intensively

studied by various groups. States of scissors type have been excited in (e,e') experiments at backward angles and are located around 2-3 MeV, while the spin-flip states are seen in (p,p') experiments at forward angles and are expected to be seen in the energy interval of 5-10 MeV. A scissors mode describes the angular oscillation of protons against neutrons; the total strength of the mode is proportional to β^2, with β denoting the nuclear deformation. Actually, this feature confirms the collective character of the mode. The sound contributions for the mentioned field were reviewed in Refs. [3, 4]. Since the M1 strength of the scissors mode is proportional to β^2,people believed for a long time that the collective magnetic bands are specific to the deformed nuclei.

This assertion is however not true since there are magnetic bands where the ratio between the moment of inertia and the $B(E2)$ value for the transition $0^+ \to 2^+$ has very large values of the order of $100(eb)^{-2}MeV^{-1}$. This feature can be justified by a large transversal magnetic moment, which induces large M1 transitions but no charge quadrupole moment[6]. A large transversal magnetic moment may be associated to a triaxial core to which a prolate-proton and an oblate-neutron orbital. The proton angular momentum is oriented along the long axis of the core while the neutron-s along the short axis. In a hydrodynamic model the core rotates along the intermediate axis. Such a configuration generates a chiral pair of $\Delta I = 1$ bands.

If the core is almost spherical then the system exhibits magnetic bands

For the chiral configuration, suppose that the three angular momenta form a right-handed trihedron. By changing the orientation of one angular momentum, one obtains a left-handed trihedron. This transformation is called a chiral transformation. If the model Hamiltonian commutes with the chiral generators, the system exhibits a chiral symmetry. As always happens the symmetry is identified when this is broken, when the energies corresponding to the right-handed frame are different from those showing up in the left-handed frame. Hence, a signature for a chiral symmetry is the appearance of two $\Delta I = 1$ bands with close energies.

Here we address the question whether the chiral configuration mentioned above consisting in one triaxial core, a particle-like proton and a hole-like neutron is a unique solution for building up a large transversal magnetic moment.

The formalism described in this paper consists in a phenomenological core with two components, proton- and neutron-bosons, and two quasiparticles having the total angular momentum oriented along the symmetry axis of the system. We investigated the possible

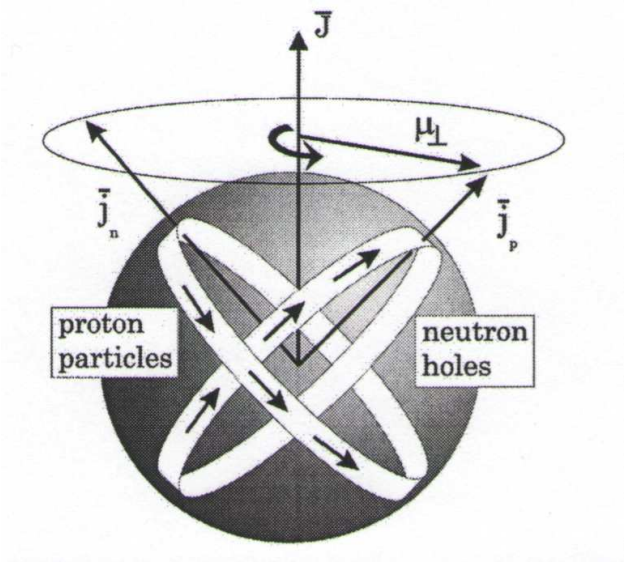

FIG. 13: Magnetic rotation. Particle-like proton and hole-like neutron move around a near spherical core. The corresponding angular momenta $\vec{j_p}$ and $\vec{j_n}$ respectively, generate a transversal magnetic moment $\vec{\mu}_\perp$ perpendicular on the total angular momentum $\vec{J}$.Due to the negative value of the neutron gyromagnetic factor the transversal components of the proton and neutron magnetic moments sum up, while the parallel components are subtracted from each other. Due to the large transversal magnetic moment, the interaction with an e.m. field may excite the system in a magnetic dipole state.

orthogonal configuration of the angular momenta carried by the mentioned components. This would be a prerequisite of a large dipole moment. The model Hamiltonian associated to the interacting particle-core system has the expression:

$$\begin{aligned} H &= H_{GCSM} + \sum_{\alpha} \epsilon_a c_\alpha^\dagger c_\alpha - \frac{G}{4} P^\dagger P \\ &- \sum_{\tau=p,n} X_{pc}^{(\tau)} \sum_m q_{2m} \left(b_{\tau,-m}^\dagger + (-)^m b_{\tau m} \right) (-)^m - X_{sS} \vec{J}_F \cdot \vec{J}_c, \end{aligned} \tag{1.38}$$

If one neglects the particle-core spin-spin term as well the scalar product $\mathbf{J_p}.\mathbf{J_n}$ comprised by H_{GCSM}, the resulting Hamiltonian exhibits a chiral symmetry. The neglected terms break the chiral symmetry. Indeed, by changing the sign of one angular momentum of the trihedron $\mathbf{JF}, \mathbf{Jp}, \mathbf{Jn}$ one obtains a Hamiltonian which differ from the initial one. Associating to each transformed trihedron a rotational band one obtains four chiral partner bands with specific symmetries. Two of these bands are degenerate. Experimental results lead to a

set of fingerprints of the chiral bands, conventionally called *twin bands*: 1) the partner bands are close in energy 2) the energy staggering function does not depend on angular momentum. 3) The ratios $B(M1)/B(E2)$ as well as $B(M1)_{in}/B(M1)_{out}$ where $B(M1)_{in}$ and $B(M1)_{out}$ denote the magnetic dipole transitions in-band and inter-band, respectively. A careful theoretical analysis show the these criteria are necessary but not sufficient, the partner bands could belong, under certain circumstances, to different nuclear shapes. These criteria have been checked in the numerical applications to ^{192}Pt, ^{188}Os and ^{190}Os. We underline the fact that the existent formalisms refer either to odd-odd or to odd-even nuclei. Our description concerns the even-even nuclei. Results of our investigations were published in the paper: **Semi-phenomenological description of the chiral bands in 188;190Os, A. A. Raduta and C. M. Raduta, J. Phys. G: Nucl. Part. Phys. 42 (2015) 065105 (16pp)** . We hope that the present paper will stimulate the extension of the experimental measurements to the even-even nuclei. Numerical results are summarized in Table 1 and Figs 1-4. Excitation energies calculated with these parameters are compared

	$\rho = d\sqrt{2}$	A_1[keV]	A_2[keV]	A_3[keV]	A_4[keV]	X'_{pc}[keV]	X_{sS}[keV]	$g_p[\mu_N]$	$g_n[\mu_N]$	$g_F[\mu_N]$	r.m.s.[keV]
^{188}Os	2.2	438.7	-93.8	-70.5	9.1	1.02	3.0	0.828	-0.028	1.289	16.93
^{190}Os	2.0	366.1	92.6	24.0	12.2	1.66	2.0	0.7915	0.0086	1.289	18.63

TABLE V: The structure coefficients of the model Hamiltonian were determined by a least square procedure. On the last column the r.m.s. values characterizing the deviation of the calculated and experimental energies are also given. The deformation parameter ρ is adimensional. The parameter X'_{pc} is related to X_{pc} by: $X'_{pc} = 6.5\eta^{(-)}_{\frac{11}{2}\frac{11}{2}} X_{pc}$.

with the corresponding experimental data, in Figs. 1,2. One notes a good agreement of results with the corresponding experimental data.

---

[1] N. Lo Iudice and F. Palumbo, Phys. Rev. Lett. **41**, 1532 (1978).

[2] G. De Francheschi, F. Palumbo and N. Lo Iudice, Phys. Rev. **C29** (1984) 1496.

[3] N. Lo Iudice, Phys. Part. Nucl. **25** , 556, (1997).

[4] D. Zawischa, J. Phys. G**24**, 683,(1998).

[5] S. Frauendorf, Rev. Mod. Phys. **73** (2001) 463.

[6] Jenkins et al., Phys. Rev. Lett. **83** (1999) 500.

[7] A. A. Raduta, A. Faessler and V. Ceausescu, Phys. Rev. **C36** (1987) 2111.

[8] A. A. Raduta, I. I. Ursu and D. S. Delion, Nucl. Phys. **A 475** (1987) 439.

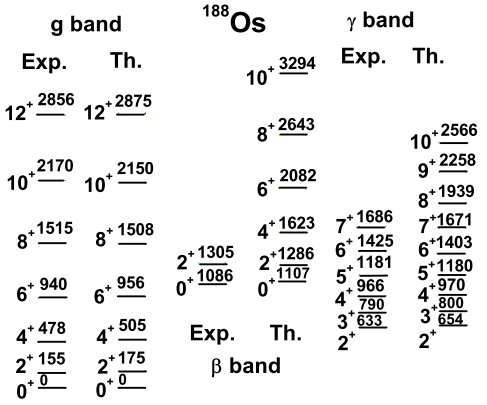

FIG. 14: Experimental (Exp.) and calculated (Th.) excitation energies in ground, β and γ bands of ^{188}Os. Data are taken from [**?**].

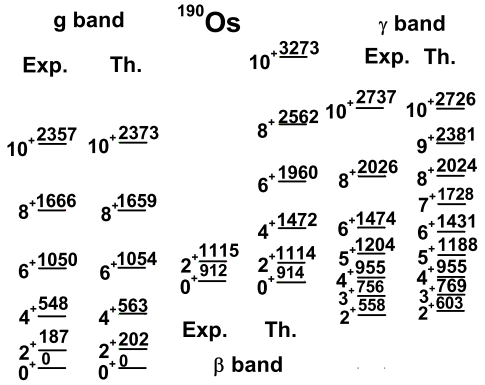

FIG. 15: The same as in Fig.1 but for ^{190}Os with data from Ref.[**?**].

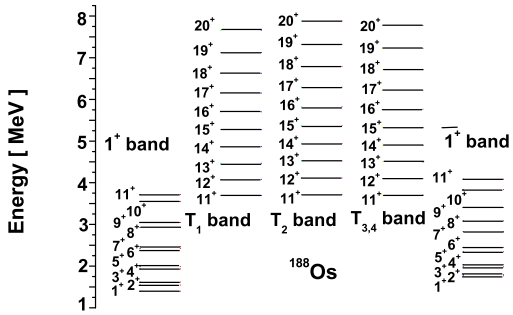

FIG. 16: Excitation energies for the yrast (lower-left) and non-yrast (lower-right) boson dipole states of ^{188}Os. The twin bands T_1 and T_2 are also shown.

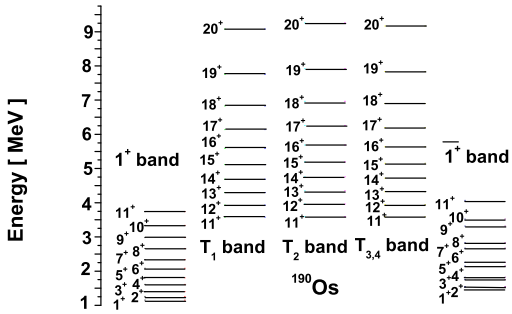

FIG. 17: The same as in Fig. 3 but for ^{190}Os. Here the dipole bands from the lower columns are described by $|1; JM\rangle$ and $|\bar{1}; JM\rangle$.

[9] A. A. Raduta and D. S. Delion, Nucl. Phys. **A 491** (1989) 24.

[10] N. Lo Iudice, A. A. Raduta and D. S. Delion, Phys. Lett. **B 300** (1993) 195; Phys. Rev. **C 50** (1994) 127.

[11] A. A. Raduta, D.S. Delion and N. Lo Iudice, Nucl. Phys. **A564** (1993) 185.

[12] A. A. Raduta, I. I. Ursu and Amand Faessler, Nucl. Phys. **A 489** (1988) 20.

[13] A. A. Raduta, A. Escuderos and E. Moya de Guerra, Phys. Rev. **C 65** (2002) 0243121.

[14] A. A. Raduta, N. Lo Iudice and I. I. Ursu, Nucl. Phys. **584** (1995) 84.

[15] A. A. Raduta, Phys Rev C **A51** (1995) 2973.

[16] A. Aroua, *et al*, Nucl. Phys. **A728** (2003) 96.

[17] A. A. Raduta, C.M. Raduta and Amand Faessler, Phys. Lett. B, 635 (2006) 80.

[18] A. A. Raduta, Al. H. Raduta and C. M. Raduta, Phys. Rev. C74 (2006) 044312.

[19] Raduta et al., Phys. Rev. C 80, 044327 (2009).

[20] A. A. Raduta, V. Ceausescu, A. Gheorghe and R. Dreizler, Phys. Lett. **B 121**1; Nucl. Phys. **A 381** (1982) 253.

[21] A. A. Raduta, A. Faessler and V. Ceausescu, Phys. Rev. **C 36** (1987) 439.

[22] A. A. Raduta, I. I. Ursu and D. S. Delion, Nucl. Phys. **A 475** (1987) 439.

[23] A. A. Raduta and D. S. Delion, Nucl. Phys. **A 491** (1989) 24.

[24] N. Lo Iudice, A. A. Raduta and D. S. Delion, Phys. Rev. **C50** (1994) 127.

[25] A. A. Raduta, C. lima and Amand Faessler, Z. Phys. A - Atoms and Nuclei **313**, (1983), 69.

[26] Coral M. Baglin, Nuclear Data Sheets 113 (2012) 1871.

III Analytical solution for the Davydov-Chaban Hamiltonian with a sextic potential and $\gamma = 30^0$

We proposed an analytical solution for a Davydov-Chaban Hamiltonian with a sextic potential for the β variable and the variable γ fixed at the value of 30^0 The resulting formalism is conventionally called the Z(4)-sextic model. The mentioned model exhibits analytical solutions for the level energies of ground and beta bands, while for the γ band levels some approximations are needed. Due to the scaling property, energies and $B(E2)$ values depend on a sole parameter modulo an integer number which fixes a limit for the number of states taken into consideration. Under certain circumstances which provide simpler potentials, energies and branching ratios are independent of any adjusting parameters. Energies and the E(2) transitions predicted by the sextic z(4)-sextic have been studied as function of one free parameter. Results for some special cases are presented in detail. Numerical applications refer to the isotopes 128,130,132 Xe and 192,194,196 Pt. A qualitative agreement with data is obtained. In the case of the Xe isotopes a phase transition is pointed out.

The work shortly described above was published in the paper: **PHYSICAL REVIEW C 91, 014306 (2015), Analytical solution for the Davydov-Chaban Hamiltonian**

with a sextic potential for = 30, P. Buganu and R. Budaca

---

[1] D. Bonatsos, D. Lenis, D. Petrellis, and P. A. Terziev, Phys. Lett. B 588, 172 (2004).

[2] A. S. Davydov and A. A. Chaban, Nucl. Phys. 20, 499 (1960).

[3] D. Bonatsos, D. Lenis, D. Petrellis, P. A. Terziev, and I. Yigitoglu, Phys. Lett. B 621, 102 (2005).

[4] A. G. Ushveridze, Quasi-Exactly Solvable Models in Quantum Mechanics (Institute of Physics Publishing, Bristol, 1994).

[5] G. L evai and J. M. Arias, Phys. Rev. C 69, 014304 (2004).

[6] A. A. Raduta and P. Buganu, J. Phys. G 40, 025108 (2013).

[7] A. A. Raduta and P. Buganu, Phys. Rev. C 83, 034313 (2011).

[8] L. Fortunato, Phys. Rev. C 70, 011302 (2004).

[9] M. E. Rose, Elementary Theory of Angular Momentum (Wiley, New York, 1957).

[10] A. S. Davydov and G. F. Filippov, Nucl. Phys. 8, 237 (1958).

[11] A. A. Raduta and P. Buganu, Phys. Rev. C 88, 064328 (2013).

IV Energy spectrum, reduced quadrupole transition probabilities and shape deformation in the even-even isotopes of 180196Pt

The even-even isotopes 180196 Pt were studied within two exactly solvable models called "Davidson and spheroidal formalism" and "Davidson si Matiew Approach (DMA)", respectively. The energies of the bands ground, beta and gamma as well as the reduced intraband and inerband probabilities and the dependence of the nuclear shape on the isotope and on the band. Numerical results are compared with the corresponding experimental data as well as with the theoretical results obtained with other methods.

The DMA method uses the Davidson potential which yields an equation for the generalized Laguere polynomials. The gamma potential is chosen such that it has a minimum at $\gamma_0 = 30^0$. Consequently the equation for the γ variable has the Mathieu function as solution. In the case of the nuclei with axial symmetry the chosen potential for γ leads to a differential equation for the spheroidal function. Numerical results are compared with both the experimental data and those obtained by the same authors through a different approach.

These results are described in the paper: **ENERGY SPECTRA, E2 TRANSITION**

PROBABILITIES AND SHAPE DEFORMATIONS FOR THE EVEN-EVEN ISOTOPES 180196 Pt, P. Buganu and A. A. Raduta,Rom. Jour. Phys. vol. 60, Nos.1-2, (2015), p.161-178.

---

[1] A. A. Raduta and P. Buganu, Phys. Rev. C 88, 064328 (2013).

[2] A. A. Raduta and P. Buganu, J. Phys. G: Nucl. Part. Phys. 40, 025108 (2013).

[3] A. A. Raduta and P. Buganu, Phys. Rev. C 83, 034313 (2011).

[4] A. Gheorghe, A. A. Raduta and A. Faessler, Phys. Lett. B 648, 171 (2007).

[5] L. Wilets and M. Jean, Phys. Rev.102, 788 (1956).

[6] L. Fortunato, Eur. J. Phys. A 26, s01, 1-30 (2005).

[7] P. M. Davidson, Proc. R. Soc. 135, 459 (1932).

[8] Dennis Bonatsos, D. Lenis, N. Minkov, D. Petrellis, P. P. Raychev, P. A. Terziev, Phys. Lett. B 584, 40 (2004).

[9] M. E. Rose, Elementary Theory of Angular Momentum (Wiley, New York, 1957).

RESULTS, 2016

Stage 6: SSD for the double beta decay and microscopic description of finite bands

I. A new renormalization procedure of the quasiparticle random phase approximation

A. A. Raduta, C. M. Raduta, Int. Jour. Mod. Phys. E 25,3 (2016) 1650017

The big merit of the liquid drop model (LDM) proposed by Bohr and Mottelson [1] is that one defined the concept of rotational bands. Also, some collective properties of spherical nuclei have been nicely described. The main drawback of LDM consists of the fact that it accounts only for the spherical and harmonic motion of the drop, while many experimental data reclaim a non-harmonic picture and, moreover, many nuclei exhibit static deformed shapes. Many phenomenological improvements have been proposed along the time, among which few are to be mentioned: a) rotation-vibration model [2]; b) Gneus-Greiner model [3]; c) generalized collective formalism [4] ; d) coherent state model [5, 6]; e) interacting boson approximation [7]. In parallel microscopic theories have been formulated, trying to get

counterparts of the phenomenological methods and interpret the nuclear collective motion in terms of the single particle motion. Thus, the random phase approximation built on the top of either the Hartree-Fock or the BCS ground state (QRPA) [8] provides a collective state which corresponds actually to the one phonon state predicted by the harmonic LDM [9]. Another important result is that of Kumar and Baranger, who calculated the inertial and stiffness parameter microscopically [10], the potential energy surface leading to some sound nuclear structure interpretation. Based on the RPA ground state, several procedures of accounting for some new correlations, i.e. of going beyond RPA, have been proposed. Such procedures are related with the equations of motion method [11–14] or boson expansion technique [15, 16, 18, 19].

The RPA method has also been extended to deformed nuclei by using a deformed mean field [20, 21] and various two body interactions with the channels of particle hole (ph), particle particle (pp) and hole-hole considered on equal footing [22]. To give an example, a fully consistent axially-symmetric deformed Hartree-Fock-Bogoliubov (HFB) + QRPA approach with the D1S Gogny interaction was used in Ref. [24] to study giant resonances in Mg and Si even isotopes. A new method for solving the Skyrme-HFB-QRPA problem in deformed nuclei was reported in Ref.[25]. Therein, the Skyrme-HFB-QRPA mean field was calculated in the coordinate-space representation. The formalism was applied for isovector and isoscalar quadrupole modes in spherical ^{20}O and deformed ^{26}Ne nuclei. The effect of deformation on the double beta decay rate [22] has been studied within a deformed pnQRPA.

A common features of all procedures involving QRPA for deformed nuclei is the use of a deformed single particle basis like Nilsson, deformed Woods-Saxon or projected spherical single particle basis [23], and the quasiparticle-quasiboson approximation is built on the top a static deformed ground state.

A procedure which keeps the appealing harmonic picture of RPA but includes in the definition of the phonon operator new correlations, is obtained by renormalizing the specific equations of motion [26]. This is achieved by considering in the commutation relations of the two quasiparticle operators not only the C-number term, which actually defines the quasi-boson approximation, but also a scalar term which is replaced by its average on the correlated ground state. The average value depends on the RQRPA amplitudes and consequently is to be determined self-consistently together with the RQRPA equations. Thus, the drawback of the standard RPA formalism of collapsing for a critical value of the attractive long range

interaction strength, is removed. Indeed, the collective root of the RPA equations goes to zero not for a finite value of the mentioned interaction strength, but only asymptotically. This approach was extended to the proton-neutron Gamow-Teller dipole interaction in Refs. [27]. We notice that going beyond the quasi-boson approximation by considering additional terms in the mutual commutation relations of the quadrupole (or dipole) two quasiparticle operators the Pauli principle, violated by the standard QRPA formalism, is to some extent restored. A more complex procedure was proposed in Ref.[28] where the RPA and BCS equations are simultaneously renormalized. As a consequence the BCS and RPA equations are coupled together and therefore are to be self-consistently solved.

Vanishing the excitation energy of the collective RPA state corresponds to a phase transition where the ground state is unstable to adding small contribution. Around this critical interaction the RPA method is no longer valid. In order to stabilize the ground state it is necessary either to change the mean field for the single particle motion, which results in having deformed single particle orbits, or to renormalize the basic equations.

A distinct renormalization procedure was proposed by Takada in Ref.[29]. The author defines two consecutive spherical Bogoliubov-Valatin (BV) transformation for treating the pairing interaction. In the second order quasiparticle representation, one builds a phonon operator including a scattering term, conventionally called as *attached* field, which allows accounting for nonlinear effects ignored in the standard QRPA. The model was tested, with positive results, for a single j-shell. Note that the second BV transformation is also spherical, i.e. the new quasiparticle operators are tensors of definite rank. Therefore the new ground state takes account of the paring correlations but not of the quadrupole-quadrupole interaction. The non-linear effects which renormalize the QRPA are due to the *attached* term and not by deforming the single quasiparticle mean-field.

In the present paper we propose a new method of renormalizing the QRPA equations. As we shall see, the result for the collective root is that it does not vanish in a critical interaction strength, where the standard QRPA collapses, but reaches a minimum value and moreover the energy increases when a subsequent increase of the strength is performed. The new point of this work is that the mean field is redefined in the quasiparticle picture by including in the ground state the quasiparticle quadrupole pairing correlations. Hence the ground state is redefined by terms of the QQ interaction and not exclusively by pairing correlations, as in Ref.[29]. As a result, both the new quasiparticles and the new QRPA

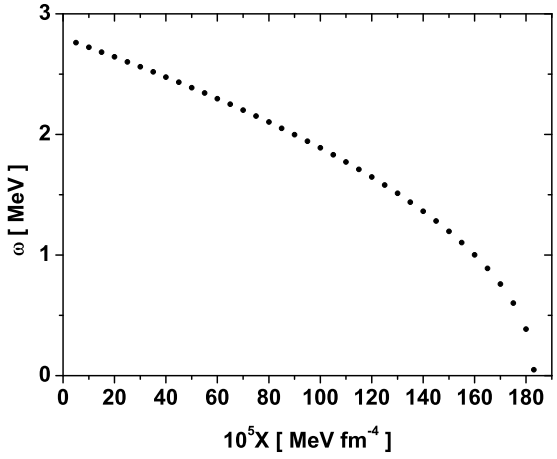

FIG. 18: The spherical QRPA energy as function of the quadrupole-quadrupole interaction strength for the case of a single shell, $j = i_{13/2}$.

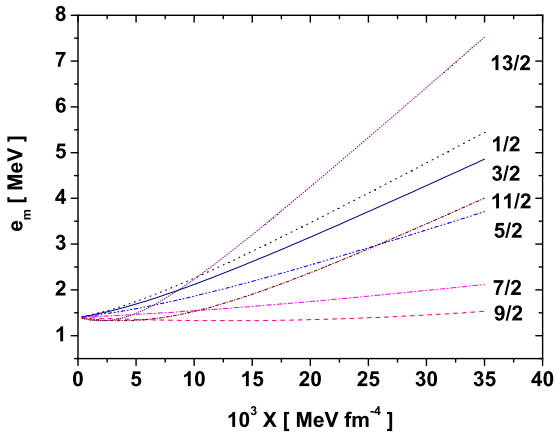

FIG. 19: The deformed quasiparticle energies for the $j = i_{13/2}$ multiplet.

solutions are deformed. Thus, we formulated an approach of renormalizing the QRPA such that no breaking down shows up. Indeed, the first QRPA energy, instead of vanishing, it becomes minimum and then, by increasing the long range interaction strength, is increasing. Things happen as if the effective interaction changes its character, from attractive to an repulsive one. The formalism redefines first the system ground state by accounting for the quasiparticle quadrupole pairing interaction. Moreover, on the top of the newly defined ground state a QRPA description is constructed. It turns out that the drawback of the standard QRPA of collapsing for a critical value of the interaction strength, is removed. In the new picture some higher QRPA dynamics is included. Indeed, the scattering terms are effectively participating in building up the new phonon operator.

We note that the new quasiparticles are not tensors of definite rank and projection. They have however a definite j. This makes the difference with the picture where first one defines a deformed mean field and then the pairing correlations are considered. In this case j is not a good quantum number, but Ω is. This difference favors the present approach, when the QRPA is supplemented by an angular momentum projection operation of the many body states.

The states considered in the present work are characterized by $K = 0$ and therefore by the total angular momentum projection, finite bands of $K = 0$ can be defined. Results are summarized in the following figures:

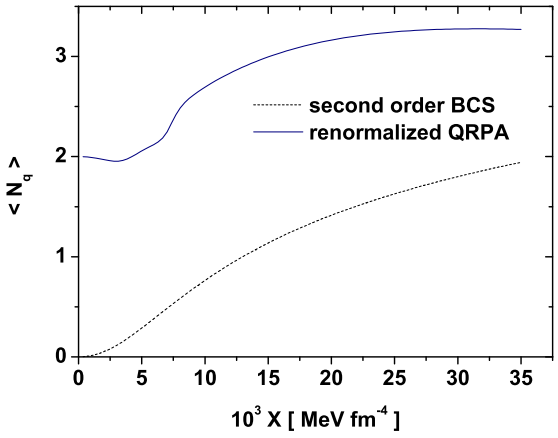

FIG. 20: The average number of quasiparticles in the second order BCS state, $|\widetilde{BCS}\rangle$.

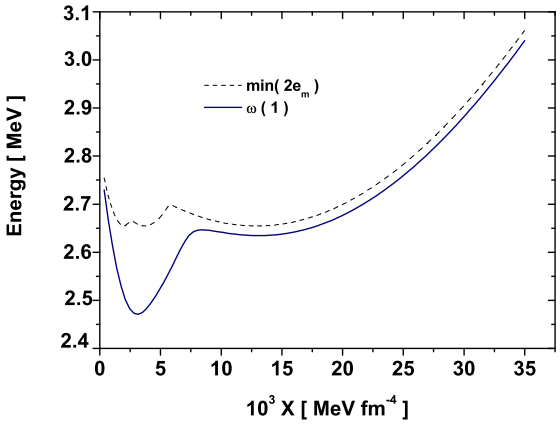

FIG. 21: The first QRPA equation root as a function of the QQ interaction strength. The minimal two quasiparticle energies are also presented as a function of X.

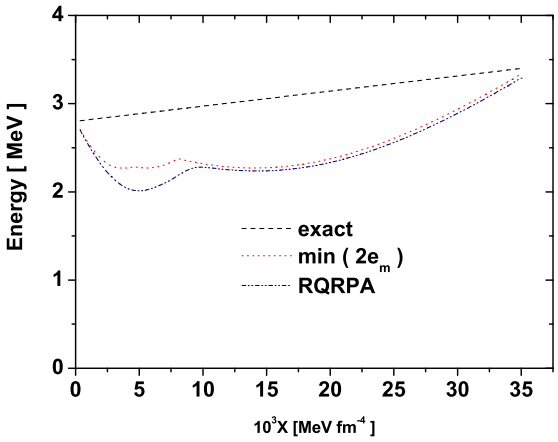

FIG. 22: The first excited state energies predicted by the renormalized QRPA are compared with the energy of the first 2^+ state, given by the exact calculation in the case of 2 nucleons moving in the single shell j=13/2. The minimal two quasiparticle energies are also presented. The three sets of energies are plotted as function of the QQ interaction strength, X. The RQRPA results correspond to $q_0 = 56fm^2$

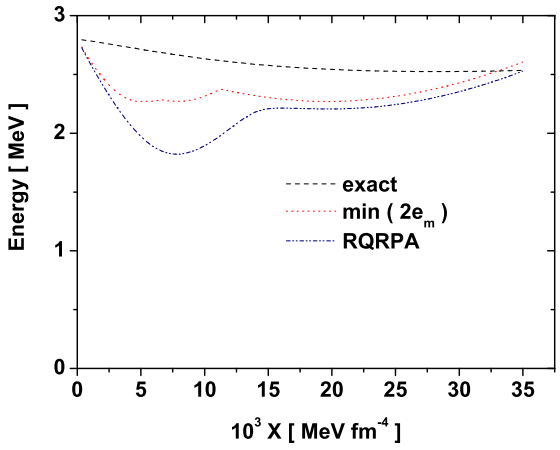

FIG. 23: The first excited state energies predicted by the renormalized QRPA are compared with the energy of the first 2^+ state, given by the exact calculation in the case of 4 nucleons moving in the single shell j=13/2. The minimal two quasiparticle energies are also presented. The three sets of energies are plotted as function of the QQ interaction strength, X. The RQRPA results correspond to $q_0 = 40fm^2$

Results were in detail described in the paper: **A new renormalization procedure of the quasiparticle random phase approximation, A. A. Raduta, C. M. Raduta, Int. Jour. Mod. Phys. E, Vol. 25,o. 3(2016) 1650017.**

---

[1] A. Bohr and B. Mottelson, Mat. Fyz. Medd. Dan. Vidensk. Selsk. **27** (1953) 16.

[2] A. Faessler and W. Greiner, Z. Physik **168** (1962) 425; **170** (1962) 105.

[3] G. Gneuss, W. Greiner, Nucl. Phys. **A171** (1971) 449.

[4] P. O. Hess, J. A. Maruhn, W. Greiner, J. Phys. **G 7** (1981) 737.

[5] A. A. Raduta, V. Ceausescu, A. Gheorghe and R. Dreizler, Nucl. Phys. **A 381** (1981) 253; Phys. Lett. **B 99** (1982) 444.

[6] A. A. Raduta, Nuclear Structure with coherent states, Springer, 2015 edition, ISBN 978-3-319-14641-6.

[7] A. Arima, F. Iachello, Ann. Phys. (N.Y.) **91** (1976) 253; Ann.Phys. (N.Y.) **123** (1976) 468.

[8] W. Greiner and J. A. Maruhn, Nuclear models, ISBN 3-540-59180-X, Springer-Verlag, Berlin, Heidelberg, New York

[9] L. S. Kisslinger, R. A. Sorensen, Rev. Mod. Phys. **35** (1963) 853.

[10] K. Kumar and M. Baranger, Nucl Phys. **A 122** (1968) 273; Baranger and K. Kumar, Nucl. Phys. **A 110** (1969) 490.

[11] A. K. Kerman and C. M. Shakin, Phys. Lett. 7 (1962) 151.

[12] G. Do Dang and A. Klein, Phys. Rev. **133** (1964) B257.

[13] A. A. Raduta, A. Sandulescu and P. O. Lipas, Nucl. Phys. **A 149** (1970) 11.

[14] A. A. Raduta and A. Sandulescu, Nucl. Phys. **A 181** (1972) 153.

[15] S. T. Belyaev and V. G. Zelevinsky, Nucl. Phys. **39** (1962) 582.

[16] T. Marumori *at al.* Prog. Theor. Phys. **31** (1964) 1009;**32** (1964) 726.

[17] B. Sorensen, Nucl. Phys. **A 97** (1967) 1; **A 119** (1968) 65, **A 142** (1970) 392.

[18] A. A. Raduta, V. Ceausescu, G. Stratan and A. Sandulescu, Phys. Rev. **C 8** (1973) 1525.

[19] A. Klein, E. R. Marshalek, Rev. Mod. Phys.**63** (1991) 375.

[20] M. Z. I. Gering and W. D. Heiss, Phys. Rev. C **29** (1984) 1113.

[21] P. Moller and J. Randrup, Nucl. Phys. A 514, (1990) 49.

[22] A. A. Raduta, Amand Faessler and D. S. Delion, Nucl. Phys. A**564** (1993) 185.

[23] A. A. Raduta, A. Escuderos and E. Moya de Guerra, Phys. Rev C **65** (2002) 0243121.

[24] S. Peru and H. Goutte, Phys. Rev. C **77** (2008) 044313.

[25] Kenichi Yoshida and Nguen Van Giai, Phys. Rev. C **78** (2008) 064316.

[26] K. Hara, Prog. Theor. Phys. **32** (1964) 88.

[27] J. Toivonen, J. Suhonen, Phys. Rev. Lett **75** (1995) 410.

[28] R. V. Jolos, W. Rybarska-Nawrocka, Z. Phys. **A 296** (1980) 73.

[29] K. Takada, Progress of Theoretical Physics, Vol 64, No. 1 (1980) 114.

II Specific features and symmetries for magnetic and chiral bands in nuclei, A. A. Raduta, Progress in Particle and Nuclear Physics, 90 (2016) 241-298

The magnetic bands have been first seen in ^{198,199}Pb. There are two mechanisms of generating angular momentum in the magnetic bands: a) the shears-like motion of the proton and neutron and the collective rotation of the core. At the beginning of the band the states have mostly a shears character, while the core contribution is about zero. Increasing the rotation frequency, the shears become closer and closer and the core's rotation generate an increasing amount of angular momentum. Correspondingly, the transversal magnetic moment of the shears blades is decreasing and finally vanishes. The magnetic bands show up due to the spontaneous breaking of the rotation symmetry for the currents distribution. The name comes from the fact that the magnetic moment is the order parameter in the phase transition generated by the mentioned symmetry breaking. The magnetic bands are finite and non-collective since only few particle participate in determining the M1 transitions.

The first nucleus suspected to be chiral was ^{134}Pr, although later on it was proved that despite the partner bands are close in energy they correspond to different shapes, which results in having different electromagnetic properties.

The field of magnetic and chiral bands developed very rapidly such that so far several nuclear mass regions, e.g. $A \sim 60, 80, 100, 130, 190, 200,$ have been intensively explored. Experimentalists formulated a set of criteria which could play the role of fingerprints for identifying the chiral bands. On the other hand theoreticians tested their approaches by requiring several conditions to be fulfilled in order to call a band doublet as chiral. In the intrinsic frame the chiral symmetry is broken. This is restored in the laboratory frame which results in having two non-degenerate bands. The degeneracy from the intrinsic frame

is removed due to the tunnelling process between states of different handedness. However, for large spin the barrier between two types of states is too high such that the tunneling is prevented and the two bands become degenerate. Thus, the chiral doublets last for a finite interval of spins. Moreover chirality is not a collective phenomenon, since it is the effect of few particle motion.

Theoretical approaches like TAC (tilted axis cranking) and PRM (particle-rotor model) have been used first for odd-odd nuclei where the chiral geometry, responsible for maximal transversal magnetic moment, consists in one high j particle-like proton and a high j hole-like neutron coupled to a triaxial rigid rotor. The interacting system is considered in the intrinsic reference frame, whose axes coincide with those of the inertia ellipsoid. The minimum energy condition is satisfied when the proton is oriented along the short axis, the neutron along the long axis, while the collective angular momentum of the core is aligned, according to the hydrodynamic model to the intermediate axis, since this has the maximum moment of inertia. Such a configuration minimizes also the Coriolis interaction, which favors the angular momenta alignment and moreover, the proton and neutron wave functions have a maximal overlap with the density distribution ellipsoid.

This concept was extended to a set of protons of particle-type and a set of neutron of hole-type coupled to a triaxial core. Other extensions referred to the odd-even and the even-even nuclei. The chiral bands are first of all, finite bands; they are close in energy, the intra-band M1 transitions are large and E2 transition small. Also, the moments of inertia in the two bands are similar or close to each other.

The chiral character of the band doublet is induced by the aplanar motion associated to the angular momentum of the valent proton-particles, hole-neutrons and triaxial rigid core which may be combined as a left- or right-handed frames. The doublet structure is a reflection of the chiral symmetry restoration in the laboratory frame.

Since in many of theoretical approaches the triaxial rigid rotor is employed for the collective core, a chapter was devoted to the semi-classical description of the triaxial rigid rotor as well as to the study of the cranked triaxial rotor, hoping that this information will be useful to the young readers. Dequantizing the quantal triaxial rotor and separating the kinetic and potential energy and then quantizing the result one finds a pair of degenerate bands of different handedness. The degeneracy is lifted up due to the tunneling through the potential barrier in the region of low spins. Increasing the spin the two bands become degenerate. The

results for planar and aplanar motion are analytically presented. The semi-classical spectrum of the triaxial rotor shows an wobbling structure in the lowest order and a nonlinear n-dependence (the number of quanta) for energies, when an approximation going beyond wobbling is adopted.

The PRM is a quantal approach which treats the system in the laboratory frame and, therefore, the double chiral members are not degenerate, while the TAC is a semi-classical procedure which first determines variationally the position of the angular momenta with respect to the density ellipsoid. TAC is able to describe the yrast band, while the coupling to the triaxial rotor or to a collective core, provides the side bands.

The angles specifying the position of the angular momentum (θ, φ) play the role of dynamic coordinates and may be used for describing the angular momentum motion. The deviation from the planar motion is described by the coordinate ϕ whose motion is softer than that of θ. The quantal equation for this coordinate is depending on the TAC solutions for the single particle motion. The corresponding potential has two symmetric minima, separated by a barrier. When the height of this barrier is small the system is tunneling from one minimum to another, which results in having an oscillatory motion, called chiral vibration. The barrier height increases with the rotation frequency and one reaches the situation when the wave function is localized in the two minima. The motion is stabilized in the two minima and that corresponds to the chiral rotation. The band degeneracy is removed and two chiral partner bands show up. If the functions are localized and the barrier is very high, the penetration is not possible any longer and the approach breaks down. To continue the description for higher spins one has to treat the correlations of the TAC trajectories through the RPA approach. An order parameter for chirality, called handedness, was defined by Grodner in Ref.[1]. The dynamic variable associated to chirality are the tilted angles specifying the orientation of the total angular momentum.

Various theoretical approaches were briefly discussed along this paper. The mean field and the two body interactions governing the many nucleon motion have been treated by cranking with deformed Woods-Saxon single particle orbits, adding the Strutinski correction, by Skyrme interaction, by relativistic covariant density functional theory, by 3D TAC and TAC+RPA. For many of experimental results these formalisms constituted efficient tools for interpreting the data. On the other hand the modern detection techniques allowed to separate bands with regular structure suspected to be of magnetic or chiral nature and thus

stimulated further improvements of the theoretical methods, increasing their capability to interpret the new data.

A new type of chiral motion in even-even nuclei was also presented, where the chiral geometry is achieved by two high j proton quasiparticles aligned to the OZ axis, coupled to a boson proton-neutron core described by the generalized Coherent State Model (GCSM). At the beginning of the chiral bands the 2qp angular momentum and the two collective angular momenta carried by the proton and neutron bosons respectively, are mutually orthogonal, which determine a large transversal magnetic moment. A particle-core type Hamiltonian is diagonalized in a basis consisting in a set of collective states of good angular momentum and a $2qp \otimes core \;\; states$, where the core's states were taken as the magnetic dipole states belonging to the band built on the scissors state 1^+. Thus one obtained four chiral bands among which two, B_2 and B_1, describe very well the experimental bands denoted by $D4$ and $D'4$ in Ref.[2], which have the fingerprints of chiral bands. The B_3 and $1'^+$ bands are mainly determined by a term proportional to $(J_p - J_n)^2$ and thereby are called as second order scissors modes. A detail comparison between this approach and that proposed by Frauendorf and Meng is presented. As we already mentioned the chiral bands appear to be a consequence of chiral symmetry restoration. This symmetry is broken in the intrinsic frame where it can be combined with other symmetry breaking as is for example the reflection-asymmetric shapes. Correspondingly in the laboratory frame both symmetries are to be restored which result in having four partner bands, two of positive and two of negative parity.

A large space was devoted to account for the actual status of the experimental measurements searching for chiral bands in various A-mass regions. There are so many publications with experimental and theoretical content so that fatally I omitted mentioning some of them. I assure the authors that this happened out of my intention.

By no means, the field of the magnetic and chiral bands is fascinating for the interesting features unveiled by both experimental and theoretical researches. The large volume of publications is a confirmation that nuclear structure is a vivid field able to produce outstanding results.

This review paper contains 22 figures, 8 tables and 174 references, and describes in 58

pages the up to date status of the field.

---

[1] E. Grodner, Acta, Phys. Pol. **B 39** (2008) 531.

[2] C. M. Petrache *et al*, Phys. Rev. **C 86**, 044321 (2012).

III. New type of chiral motion in even-even nuclei: the case of ^{138}Nd, A. A. Raduta, Al. H. Raduta and C. M. Petrache, J. Pjys. G: Nucl. Part. Phys. 43 (2016) 095107

In this paper we described a particle-core formalism for the chiral bands. The application is made for ^{138}Nd, where some experimental data are available [2, 3]. The phenomenological core is described by the GCSM. Particles move in a spherical shell model mean-field and alike nucleons interact among themselves through pairing. The outer particles interact with the core by a spin-spin force. The model Hamiltonian was treated within a restricted space associated to the phenomenological core and the subspace of aligned two proton quasiparticle states, from the $h_{11/2}$ sub-shell, coupled to the states of the phenomenological scissors-like dipole states.

The eigenvalues of the model Hamiltonian within the particle-core subspace are arranged in four bands denoted by B_1, B_2, B_3 and B_4, respectively. The bands B_3 and B_4 correspond to the particle-core states transformed by changing $\mathbf{J_p} \to -\mathbf{J_p}$ and $\mathbf{J_n} \to -\mathbf{J_n}$ respectively and are degenerate. Energies as well as the $M1$ and the E2 transition rates for these bands are quantitatively studied. The results of our calculations confer the character of chiral doublet partners to the bands B_1 and B_2.

Also, the intra-band $B(M1)$ values are large and vary when one passes from one band to another. On the contrary, the $B(E2)$ values do not depend on band and in general are small. The energy spacing in all four bands is almost constant. This is reflected by the associated energy staggering functions shown in Fig. 25. As a matter of fact these properties confer the bands B_1 and B_2 a chiral character. The bands B_2 and B_1 describe the experimental bands $D4$ and $D'4$ of ^{138}Nd.

Our work proves that the mechanism for chiral symmetry breaking, proposed in Ref. [1], which also favors a large transverse component for the dipole magnetic transition operator,

is not unique.

Note that the bands B_3, B_4, as well as the partner bands associated to the collective bands describing the core, emerge from their sister bands by considering the contribution of the collective term $(\mathbf{J_p} - \mathbf{J_n})^2$. Recalling that such term determines the excitation energy of the scissors mode, we can call the mentioned doublet members as the second order scissors bands.

In order to compare the present approach to the existent formalisms, we have to remember few specific features of the preceding procedures. For odd-odd nuclei several groups identified twin bands in medium mass regions [7–10] and even in heavy mass regions [11–13]. The formalisms proposed for these bands were based either on the Tilted Axis Cranking (TAC) approach [14] or on the two quasiparticle-triaxial rotor coupling model [15–18]. Although the efforts were mainly focused on identifying and describing the chiral twin bands in odd-odd nuclei, few results for even-odd [19–24] and even-even [25] nuclei were also reported.

Also, it is worth mentioning another boson description of the chiral phenomenon, which uses the interacting boson-fermion-fermion model (IBFFM-1) [26–29]. This hinges on the interacting boson model(IBM-1)(where there is no distinction between proton bosons and neutron bosons) for even-even nuclei and IBFM-1 for odd-A nuclei. The vibrational and rotational degrees of freedom are taken into account in describing the core by the Interacting Boson Model (IBM) with O(6) dynamical symmetry which resulted in proposing a dynamic chirality with the shape fluctuation [27]. Within the IBFFM-1, a triaxial shape is obtained by adding to the IBM1 Hamiltonian, describing the even-even core, a cubic (three-body) term. Also, it was shown that an important improvement of the agreement between the calculated and corresponding experimental data in the odd-A nuclei, is obtained if the exchange effect is accounted for. This effect reflects the anti-symmetrization of the odd nucleon and the nucleons involved in the boson structure. Within the IBFFM-1[28] the dynamic chirality in ^{134}Pr was also studied. The analysis of the wave functions has shown that the possibility for angular momenta of the valence proton, neutron and core to find themselves in the favorable, almost orthogonal geometry, is present but not dominant. Such behavior is found to be similar in nuclei where both the level energies and the electromagnetic decay properties display the chiral pattern, as well as in those where only the level energies of the corresponding levels in the twin bands are close to each other. The difference in the structure of the two types of chiral candidates nuclei can be attributed to different

β and γ fluctuations, induced by the exchange boson-fermion interaction of the interacting boson fermion-fermion model, i.e. the anti-symmetrization of odd fermions with the fermion structure of the bosons. In both cases the chirality is weak and dynamic. The interacting boson-fermion model was extended by including broken proton and broken neutron pairs [30]. The application to ^{136}Nd showed a very good agreement with experimental data for eight dipole bands, including the high spin region.

The formalism proposed in the present paper concerns the even-even nuclei and is based on a new concept. Indeed, there are few features which are different from the main characteristics of the model proposed by Frauendorf for odd-odd nuclei [1, 14]. Indeed, here the right- and left-handed frames are the angular momentum carried by two aligned protons and by proton and neutron bosons respectively, associated to the core. Within the model proposed by Frauendorf, the shears motion is achieved by one proton-particle and one neutron-hole, while here the shears blades are the proton and neutron components of the core. The $B(M1)$ values are maximal, in the Frauendorf's model, at the beginning of the band and decrease with angular momentum and finally, when the shears are closed, they are vanishing since there is no transverse magnetic momentum any longer. By contrast, in the present formalism the $B(M1)$ values increase with the angular momentum. In both models the dominant contribution to the dipole magnetic transition probability is coming from particles sub-system. This property is determined by the specific magnitudes of the gyromagnetic factors associated to the three components of the system. Due to the fact that only few particles participate to determining the quantitative properties, the chiral bands seem to be of a non-collective nature. Since the two schematic models reveal some complementary magnetic properties of nuclei, they might cover different areas of nuclear spectra.

The results are presented in a synthetic manner in the figures and table which follow.

	B_1 band			B_2 band			B_3 band			B_4 band		
I	B(M1)	$A_{pn}^{(I)}$	$A_F^{(I)}$	B(M1)	$A_{pn}^{(I)}$	$A_F^{(I)}$	B(M1)	$A_{pn}^{(I)}$	$A_F^{(I)}$	B(M1)	$A_{pn}^{(I)}$	$A_F^{(I)}$
11^+	0.662	-1.041	2.705	3.352	-1.041	-2.705	1.931	0.138	2.705	1.574	-0.138	2.705
12^+	1.664	-0.989	3.629	5.093	-0.989	-3.629	3.376	0.131	3.629	2.922	-0.131	3.629
13^+	2.596	-0.933	4.231	6.365	-0.933	-4.231	4.526	0.123	4.231	4.027	-0.123	4.231
14^+	3.409	-0.886	4.665	7.358	-0.886	-4.665	5.460	0.117	4.665	4.938	-0.117	4.665
15^+	4.109	-0.847	4.996	8.151	-0.847	-4.996	6.229	0.112	4.996	5.694	-0.112	4.996
16^+	4.711	-0.813	5.256	8.796	-0.813	-5.256	6.868	0.108	5.256	6.328	-0.108	5.256
17^+	5.231	-0.784	5.465	9.325	-0.784	-5.465	7.405	0.104	5.465	6.863	-0.104	5.465
18^+	5.681	-0.758	5.637	9.762	-0.758	-5.637	7.857	0.100	5.637	7.317	-0.100	5.637
19^+	6.071	-0.734	5.777	10.123	-0.734	-5.777	8.239	0.097	5.777	7.702	-0.097	5.777

TABLE VI: The magnetic dipole proton-neutron and fermion transition amplitudes for the bands B_1, B_2, B_3, B_4.

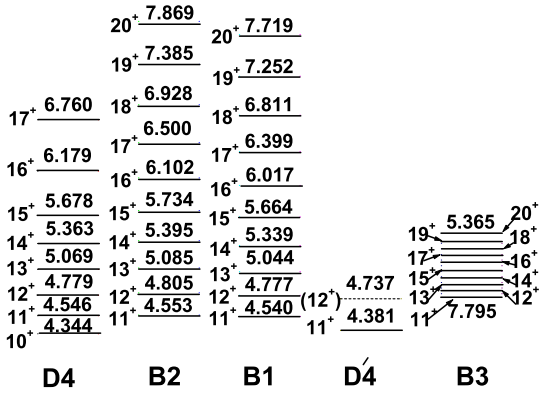

FIG. 24: The excitation energies, given in MeV, for the bands B_1, B_2, B_3 and B_4. The experimental chiral partner bands $D4$ and $D'4$ are also shown. The band B_2 is to be compared with the experimental band $D4$, while B_1 with $D'4$.

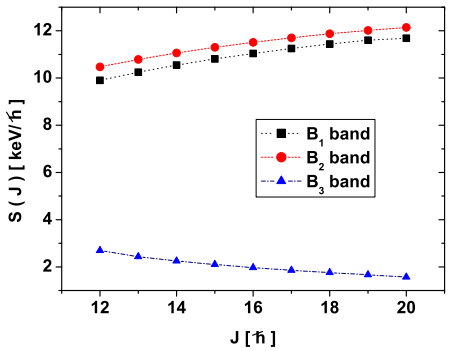

FIG. 25: The energy staggering function given in units of $keV/\hbar$, is represented as function of J for the partner bands B_1 and B_2 as well as for the band B_3.

[1] S. Frauendorf, Rev. Mod. Phys. **73**, 463 (2001).

[2] C. M. Petrache *et al*, Phys. Rev. **C 86**, 044321 (2012).

[3] H. J. Li *et al*, Phys. Rev. **C 87**, 057303 (2013).

[4] A. A. Raduta, *Nuclear Structure with Coherent States*, Springer, ISBN 978-3-319-14641-6, Cham Heidelberg New York Dordrecht London.

[5] E. Grodner, Acta Physica Polonica **B 39**, No. 2, 531 (2008).

[6] J. Deslauriers, S. C. Gujrathi, S. K. Mark, Z. Phys. **A 303**, 151 (1981).

[7] C. M. Petrache *et al.,* Nucl. Phys. **A597**, 106 (1996).

[8] A. J. Simon *et al.,* Jour. Phys. G: Nucl. Part. Phys **31**, 541 (2005).

[9] C. Vaman, *et al.*, Phys. Rev. Lett. **92**, 032501 (2004).

[10] C. M. Petrache, *et al.*, Phys. Rev. Lett. **96**, 112502 (2006).

[11] D. L. Balabanski, *et al.,* Phys. Rev. C **70**, 044305 (2004).

[12] S. Frauendorf and J. Meng, Nucl. Phys. **A 617**, 131 (1997).

[13] V. I. Dimitrov, S. Frauendorf and F. D onau, Phys. Rev. Let. **84**, 5732 (2000).

[14] S. Frauendorf, Nuclear Physics **A677**, 115 (2000)

[15] H. Toki and Amand Faessler, Nucl. Phys. **A 253**, 231 (1975).

[16] H. Toki and Amand Faessler, Z. Phys.. **A 276**, 35 (1976).

[17] H. Toki and Amand Faessler, Phys. Lett. **B 63** (1976) 121.

[18] H. Toki, H. L. Yadav and Amand Faessler, Phys. Lett. **B 66**, 310 (1977).

[19] S. Zhu *et al.* Phys. Rev. Lett. **91** , 132501 (2003)

[20] J. A. Alcantara-Nunez *et al.*, Phys. Rev. **C69** 024317 (2004).

[21] J. Timar *et al.*, Phys. Lett. **B 598**, 178 (2004).

[22] J. Timar *et al.*, Phys. Rev. **C 73**, 011301 (R) (2006).

[23] Y. X. Luo, *et al.*, Chin. Phys. Lett. **B 26**, 082301 (2009).

[24] A. D. Ayangeakaa *et al.*, Phys. Rev. Lett. **110**, 172504 (2013).

[25] E. Mergel *et al.*, Eur. Phys. J. **A 15**, 417 (2002).

[26] D. Tonev, *et al.,* Phys. Rev. Lett. **96** (2006) 052501.

[27] D. Tonev, *et al.*, Phys. Rev. C **76** (2007) 044313.

[28] S. Brant, D. Tonev, G. de Angelis and A. Ventura, Phys. Rev. C **78** (2008) 0343301.

[29] S. Brant and C. M. Petrache, Phys. Rev. C **79** (2009) 054326.

[30] D. Vretenar *et al.*, Phys. Rev. **C 57**, 675 (1998).

C. The participation of the young researchers

As results form the list of publications regarding the subjects of the project, the young researchers Radu Budaca and Petrica Buganu are coauthors of several papers. Also the two young researchers attended international conferences where presented oral communications or posters.

D. Difficulties encountered: None

E. Economic and social impacts.

The performed researches have a fundamental character. Thereby the final product is the knowledge. As results form the present report as well as form the attached papers the advanced hypotheses are 100% original and because of that the added value for the team activities represent an important contribution to the knowledge development in the field as well as to enriching the Romanian scientific creative treasure. We believe that our results will have a positive international echo and thus the Romanian science visibility will be improved. Also the obtained results contribute to creating a proper academic climate for coming topical research in he field. An example on this line is the training of the young researchers belonging to the project team. It is interesting to notice that when the project began the two young people where beginner doctorands. In the meantime they defended their PhD thesis, won the competition for scientific researcher which allowed them to be permanently employed in the Department of Theoretical Physics of IFIN-HH. Moreover in 2013 they were promote to the functions of Principal Researcher of rank III. The reason was that they have an important number of publications in the major international journals. These data prove that the atmosphere in the group of Prof. Dr. Apolodor Raduta is encouraging for young researchers in a complex and difficult field.

F. Dissemination, mobility

The team members attended several international conferences where presented invited

lectures, communications and posters. Here is the list of conferences and contributions:

1) International conference "Nuclear Structure and related topics", Dubna 2012. There Prof. A. A. Raduta presented the lecture *FRpnQRPA approach with the gauge symmetry restored. Application for the* $2\nu\beta\beta$ *decay.* The lecture appeared in the conference proceedings

2) Dynamics of open nuclear systems, Predeal, 2012.

At this conference we had several oral presentations:

a) Invited lecture (Prof. Dr. A. A. Raduta):$2\nu\beta\beta$ *decay within a higher pnQRPA approach with the gauge symmetry preserved*

b) Communication (Dr. R. Budaca): *A semi-microscopic approach to the back-bending phenomena in even-even nuclei*

c) Communication (Dr. P. Buganu): *Towards a new solvable model for the even-even triaxial nuclei*

These works have been published in the conference proceedings.

3) European Conference on Nuclear Physics,Bucharest, September 16-21,2012.

At this conference we had two lectures and two communications:

a) Invited lecture (Prof. Dr. A. A. Raduta): *Description of various nuclear phases within the Coherent State Model*

b) Invited lecture (Prof. Dr. A. A. Raduta):*New results for* $2\nu\beta\beta$ *decay within a FRpnQRPA approach with the gauge symmetry restored.*

c) Communication (Dr. R. Budaca):*Semi-microscopic description of the back-bending phenomena in deformed even-even nuclei.*

d) Communication (Dr. P. Buganu): *Toward a new description of triaxial nuclei.*

Finally the following features are to be mentioned:

i) All presentations are directly related to the subjects considered in our project.

ii) At these conferences Prof. Dr. A. A. Raduta was chairman at one morning session (Dubna) and two afternoon sessions (conferences 2 and 3 in the list)

The communicated papers have been published in the conferences proceedings:

1) A semi-microscopic approach to the back-bending phenomena in even-even nuclei,A A Raduta and R Budaca,Journal of Physics:EPJ WEB, Conference Series 413 (2013) 012028.

2) Towards a new solvable model for the even-even triaxial nuclei, A. A. Raduta and P. Buganu,Journal of Physics:EPJ WEB Conference Series 413 (2013) 012029.

3)FRpnQRPA approach with the gauge symmetry restored. Application for the 2 decay, A. A. Raduta and c. M. Raduta, EPJ Web of Conferences 38, 14003 (2012).

4)FRpnQRPA APPROACH WITH THE GAUGE SYMMETRY RESTORED. APPLICATION FOR THE 2 DECAY , A. A. Raduta,(c) Rom.Journ. Phys., Vol.57,nr. 1-2, pp. 442-471, 2012

5) $2\nu\beta\beta$ decay within a higher pnQRPA approach with the gauge symmetry preserved, A. A. Raduta, and C. M. Raduta, Journal of Physics: Conference Series 413 (2013) 012014.

Posters

1. Application of the sextic oscillator potential together with Mathieu and spheroidal functions for triaxial and X(5) type nuclei , Apolodor A. Raduta and Petrica Buganu, Firenze Conference, Italy, 2013,EPJ Web of Conferences 66, 02086 (2014), DOI: 10.1051/epjconf/ 201 4 66020 86.

2. Semi-microscopic description of the proton- and neutron-induced back-bending phenomena in some deformed even-even rare earth nuclei, R. Budaca and A. A. Raduta, Firenze Conference Italy, 2013, EPJ Web of Conferences 66, 02017 (2014), DOI: 10.1051/epjconf/ 201 4 6602017.

Invited lectures at the Balcanic Conference, 2013

1. Radu Budaca, The 13th International Balkan Workshop on Applied Physics, Constanta, Romania, 4-6 July 2013.

2.Petrica Buganu, The 13th International Balkan Workshop on Applied Physics, Constanta, Romania, 4-6 July 2013. These lectures where included in the proceedings.

Attending conferences, working stage abroad

1) Prof. Dr. Apolodor Raduta, Institut fur Theoretische Physik der Universitaet, Tuebingen, Germany, 3 months starting with 1.05.2011.

2) Prof. Dr. Apolodor Raduta, Institut fur Theoretische Physik der Universitaet, Tuebingen, Germany, 3 months starting with 1.09.2013.

3) On 5.11.2013, being invited by Tuebingen University Prof. dr. Apolodor Raduta presented the lecture "Fascinating physics of neutrinos as a severe test of some modern

theories." This was the first lecture in the series (of 6 lectures), named Humboldt lectures, for the academic year 2013-2014. It is to be noted that the lecture subject is one of those included in the project ID-2-2011.

4) Dr. Radu Budaca, International Conference on Nuclear Physics, Firentze, Iune, 2013.

5) Dr. Petrica Buganu, International Conference on Nuclear Physics, Firentze, Iune, 2013.

6) Dr. Petrica Buganu, 7th Workshop on shape phase transitions and critical point phenomena in nuclei, March 2014, Sevillia, Spain. Here he had two oral presentations:

i. Phenomenological description of triaxial nuclei.

ii. Phase transitions within some solvable models.

7) In the period of 16.09-24.09.2014, Dr. Radu Budaca attended the International school of Nuclear Physics, 36th course Nuclei in the Laboratory and in the Cosmos Erice-Sicily, Italy.

8) In period of 20.11.2014-22.11.2014, Dr. Radu Budaca participated at the TIM14 Physics Conference -Physics without frontiers, Timisoara. At this conference he presented orally the work: Quartic oscillator potential in the -rigid regime of the collective geometrical model.

G. Promoting to a higher position

1) Radu Budaca was promoted to the position of Scientific Researcher of rank III.

2) Petrica Buganu was promoted to the position of Scientific Researcher of rank III.

28.11.2016 **Prof. Dr. Apolodor Raduta**